*Faculty **of** Science*

Application of High Resolution Mass Spectrometric Methods in a Study of the Metabolome of *Trypanosoma brucei*

A THESIS PRESENTED FOR THE DEGREE OF MASTER IN PHILOSOPHY

By

RUWIDA KAMOUR

(BPharm)

[2009-2010]

This thesis is the result of the author's original research. It has been composed by the author and has not been previously submitted for examination which has led to the award of a degree.

DEDICATION

This piece of work is dedicated to my sisters

Mariam and Rokaya

As they have dedicated their time and love to me forever.

ACKNOWLEDGEMENTS

I owe my deepest gratitude to Dr Dave Watson for his assistance in making this project successful. I do appreciate his help in providing me with advice and suggestions. I am deeply grateful to The Libyan Higher Education Committee for providing me with this invaluable opportunity to study abroad and support me in all living needs starting from the academic fees to medical insurance they cover. In addition, I would like to thank the Biomedical Science Centre of Glasgow University for giving the chance to use their facilities and tremendous appreciation goes to Professor Michael Barrett for his help and advice and for everyone in the Department of Parasitology especially Jana Anderson for her help. Also I would thank RuAngelie Edrada-Ebel for helping consistently.

I am also indebted to many of my colleagues who supported me especially Leon, Mohamed, Lynsey and Alex.

Last but certainly not least, I am grateful to all my family members for their belief in me and help to make all my dreams come true.

Abbreviations

ACN	Acetonitrile
BSF	Bloodstream forms
CE	Capillary electrophoresis
CE-MS	Capillary electrophoresis-mass spectrometry
CID	Collision-induced dissociation
DESI	Desorption electrospray ionization
DMSO	Dimethyl sulfoxide
EESI	Extractive electrospray ionization
EI	Electron impact
EOF	Electro-osmotic flow
ESI	Electrospray ionization
FCS	Foetal calf serum
GC-MS	Gas chromatography-mass spectrometry
HILIC	Hydrophilic interaction liquid chromatography
HPLC	High performance liquid chromatography
IMMS	Ion mobility mass spectrometry
LC-MS	Liquid chromatography-mass spectrometry
LTQ	Linear quadrupole ion trap
MALDI	Matrix Assisted Laser Desorption Ionization
NMR	Nuclear magnetic resonance
PBS	Phosphate buffer solution
PCA	Principal component analysis
PCF	Procyclic forms
PLS	Partial least square
RP	Reversed phase
TIC	Total ion chromatogram
TOF	Time-of-Flight
TQMS	Tandem quadrupole mass spectrometry

Table of contents

List of Figures — Page

List of Tables

Abstract

Advances in analytical technologies have permitted development of new approaches to measuring living organisms' responses to environmental stimuli. Metabolomics aims to measure as many as possible of the metabolites present in an organism's metabolome. It can help biologists and pharmacologists to monitor biological responses to a drug or to disease. Nuclear magnetic resonance (NMR) spectroscopy and mass spectrometry (MS) are the most widely used techniques in the field of metabolomics. In this thesis the recent advances in metabolomics techniques are reviewed as well as recent applications of metabolomics. The practical part of the work focuses on three different metabolomic experiments. Firstly, glycolysis in bloodstream forms (BSF) of *Trypanosoma brucei* was studied through labelling its metabolome with $^{13}C_6$-labelled glucose. The labelled metabolites were identified by a combination of hydrophilic interaction chromatography interfaced with an Orbitrap mass spectrometer and by gas chromatography-mass spectrometry. Another metabolomics experiment was carried out using deuterated water to culture *T. Brucei* in order to find some answers to the unexpected pathways of this protozoan which were obtained from the $^{13}C_6$-glucose experiment, however the findings did not fully answer the questions regarding the biosynthesis of $^{13}C_3$-labelled succinate . Finally the effects of a highly active trypanocidal sample of propolis, which is naturally produced by honey bees, was studied on the BSF of *T. brucei* where it was found to produce some selective changes in the *T.brucei* metabolome thus seeming promising as a selective anti-trypanosomal agent.

CHAPTER [1]

GENERAL INTRODUCTION

1. Introduction:

The study of metabolic pathways has helped researchers to predict disease progression and the effectiveness of its treatment. Therefore, there has been an increasing potential for describing metabolic profiles in order to support the development of new medications. Metabolic profiling has developed into the more global technique of metabolomics. Metabolomics is a biological approach to identify and quantify all metabolites in all biochemical pathways comprehensively. It has been developed in order to study and measure changes in intermediate products (metabolites) such as amino acids and sugars under any conditions such as drug treatment, environmental perturbation or genetic modification (Harrigan *et al*., 2008).

The approach of using metabolic profiling in the screening, diagnosis and measurement of health started to be widely used in the 1960 s (Cunnick *et al*., 1972; Mroczek *et al*., 1972). This has lead to the application of this approach in clinical trials either to study the effectiveness of some drugs or in the development of new drugs. The application of this technique in human studies was proposed and Beecher claimed that 2000 major metabolites would appear to be a good estimate of the number of metabolites occurring in humans (Beecher, 2003).

The rapid increase in trials in this field led to two approaches, metabolic profiling and metabolic fingerprinting (Dettmer and Hammock, 2004; Ohta *et al.*, 2010). The former measures the metabolites of a selected biochemical pathway or several biochemical pathways whereas the latter compares changes in metabolic patterns in response to a disease or a drug. There is also another approach, metabolic footprinting, in which changes in metabolite patterns in a controlled growth medium are measured. Both fingerprinting and metabolic profiling can be used to find new biomarkers (Dettmer *et al*., 2007). Hence metabolomics can give valuable data for biomarkers that can be used in measurement of health, disease or the outcomes of pharmacological treatment.

Generally, there is huge number of metabolites present in biological systems due to the diversity of metabolic pathways. Therefore, the technology used must ideally provide both identification and quantification of these metabolites. However, it is extremely difficult to apply a single technique to achieve this goal. Consequently, multiple instruments using variable analytical methods are required in order to determine all the metabolites in a metabolome (Sawada *et al.*, 2009). The detailed metabolic profiling of hundreds of samples is a great challenge for analysts these days as comprehensive analysis and high throughput are difficult to achieve at the same time.

There are two different technical approaches applied in the field of metabolomics, non-targeted and targeted. The non-targeted approach enables analysts to identify a broader metabolite range and identify biomarkers. However, it is time consuming to study all data from different instruments (Sawada *et al.*, 2009). On the other hand, the targeted approach allows the analyst to look for certain types of metabolites such as amino acids in a sample which are matched to standard signals in the library of the instrument (Viant, 2008) or metabolite databases. The standard technique for targeted metabolomics is tandem quadrupole MS (TQMS) (Sawada *et al.*, 2009). Untargeted metabolomics is based on NMR, MS and other techniques such as chromatography and CE (Wu *et al.*, 2009). In addition, it needs advanced computation methods in terms of automation, computer databases and software for handling the data obtained.

1.1. Applications of NMR in metabolomic studies

NMR is used in the field of metabolomics to generate comparable data sets. Samples can be introduced into the instrument directly or after extraction. Then an NMR spectrum is obtained and compared with NMR spectra of other samples or standard samples. It can detect a high number of compounds from a high-throughput runs; intensities of measurements can be correlated to concentrations; simple sample preparation can be used and there is high reproducibility of inter-and

intra- laboratory results (Keun *et al.*, 2002; Krishnan *et al.*, 2004). However, this is highly dependent on the experimental parameters. However, NMR is less sensitive than MS which can detect molecules present in very small amounts (Harrigan *et al.*, 2008). Interpretation of the data acquired from NMR is not easy. Therefore, statistical methods such as principal component analysis (PCA) and partial least squares (PLS) are needed to generate a meaningful data for metabolomics from NMR data (Stoyanova and Brown, 2001; Gavaghan *et al.*, 2002).

1.2. Mass Spectrometry (MS):

1.2.1. Ionization techniques

Various ionisation techniques can be applied in metabolomics studies. In order to get full coverage of the metabolome more than one technique may be required.

1.2.1.1. Electrospray ionization (ESI):

The sample needs to be dissolved in a polar volatile solvent where it is transported through a needle of high potential. The sample between needle and the mass spectrometer inlet will form a Taylor cone which consists of a charged aerosol resulting from the high potential applied to the needle (1-4kV), figure 1.1. These droplets will be ejected towards the inlet capillary under the electric field. Fluid will evaporate under the effect of a warm nitrogen flow leading to formation of ions which are transferred to the high vacuum region of the mass analyzer. ESI has good sensitivity in addition to only requiring simple sample preparation procedures. However, it is sensitive to matrix effects (pH, solvent composition and salt concentration) which might lead to signal suppression. It is a mild technique that does not fragment the molecular ion. The possibility of creating ions at atmospheric pressure and in the presence of a continuous fluid flow made it compatible with HPLC (Ekman *et al.*, 2009).

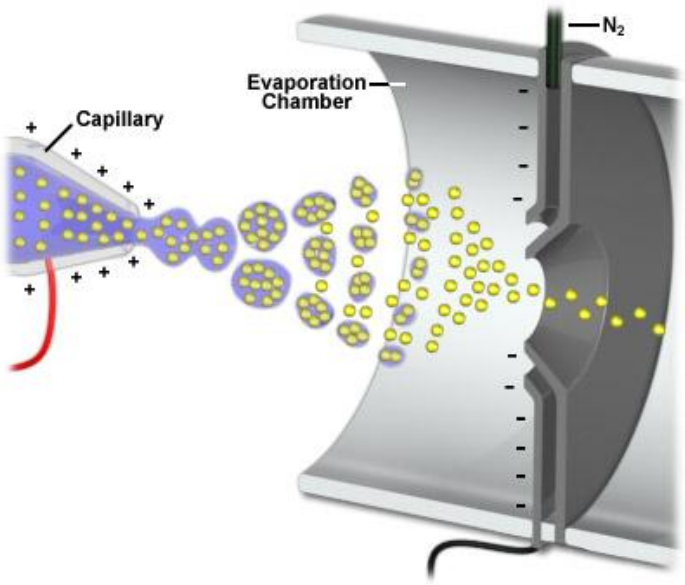

Figure 1.1: Ionization process of ESI.

1.2.1.2. Electron Impact Ionization (EI):

In EI mode ions are generated by collision of sample vapour with an electron beam. Then molecules become charged upon the removal of one electron resulting in a positively charged radical cation molecular ion. EI can only be utilized to generate positive ions. This technique results normally in fragmentation of molecular ions which in turn helps in elucidating their structure. These fragmentation patterns are instrument independent but relatively reproducible (Ekman *et al.*, 2009). Operating EI at high energy (70eV) enhances sensitivity and spectra obtained at this energy level are comparable between instruments. In most cases the concentration of $M^{+\cdot}$ is very low whereas concentration of stable fragments is high. (Hubschmann, 2009). EI is commonly utilized in GC-MS analysis.

1.2.1.3. Matrix Assisted Laser Desorption Ionization (MALDI):

In MALDI the sample is mixed or coated with a matrix and ionisation is carried out using a laser beam (Figure 1.2). MALDI is widely applied for the analysis of

polymers such as proteins and peptides. It has high throughput capacity and higher tolerance for salts than ESI. It is usually used for targeted analysis of high molecular weight metabolites. Determination of lower molecular weight metabolites is more difficult because of the substantial chemical background signals created by the matrix (Bedair and Sumner, 2008). MALDI has been used for imaging MS (IMS) of proteins in tissues (Qizhi Hu *et al.*, 2005).

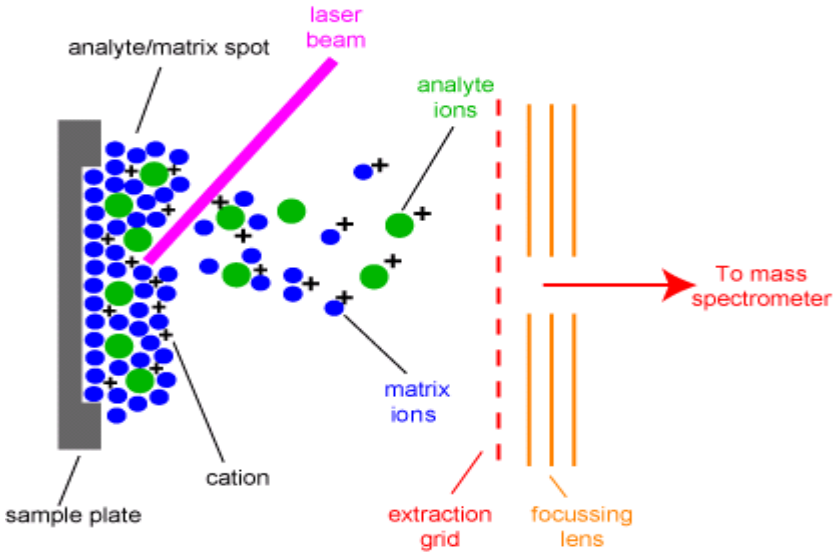

Figure1.2: Diagram of the ionization process in MALDI. http://www.chm.bris.ac.uk/ms/theory/maldi-ionisation.html

1.2.1.4. Desorption electro spray ionization (DESI):

DESI is a combination of ESI and desorption ionization. It utilizes an electrospray emitter to generate a spray of charged microdroplets which is oriented towards a sample surface. As a result, surface molecules are desorbed, ionized, desolvated and finally sent to the MS inlet. This technique does not require sample preparation. Therefore, animal and plant tissues can be directly analysed. However, experimental conditions must be optimized according to type of the sample and that may consume time. DESI ionizes both small molecules and macromolecules. Although, it has higher tolerance to sample matrix effect than ESI, its quantitative precision for solutions is less than that of ESI (Bedair and Sumner, 2008).

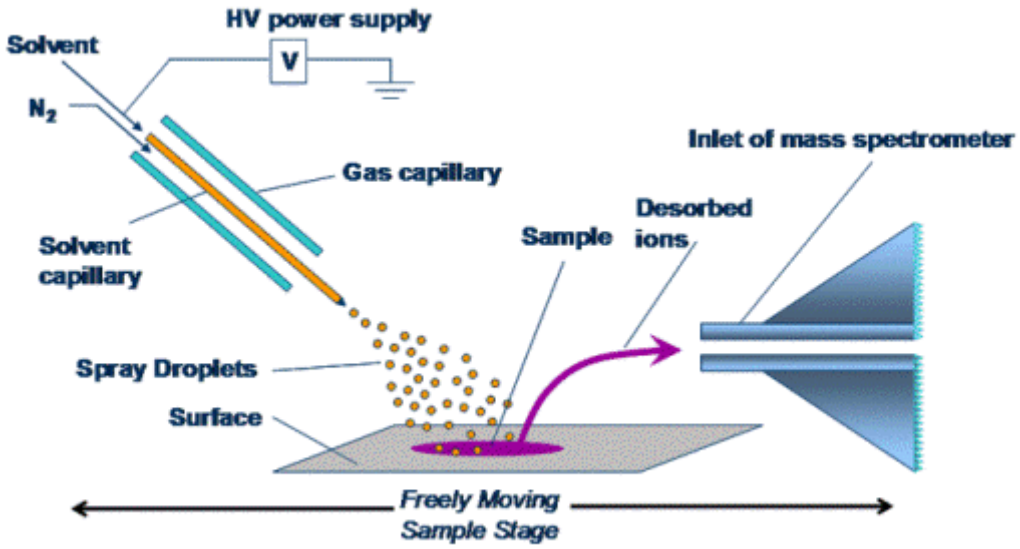

Figure 1.3: DESI. http://www.prosolia.com/DESI.html

1.2.1.5. Extractive electrospray ionization (EESI):

In EESI mode one spray is used for the sample and another for the charged microdroplets of ionizing reagent which is usually acidic aqueous methanol. The molecules of the sample are ionized after collision and then mass analyzed. Spray derived from untreated samples is stable for a long time and the technique is applicable for analysing huge number of samples (Bedair and Sumner, 2008).

1.2.2. Mass analyzers:

A range of mass analysers can be used to separate the ions generated from metabolomics samples.

1.2.2.1. Time-of-Flight (TOF)

In TOF separation the generated ions are accelerated towards the detector through a long drift tube. Therefore, TOF separates ions according to time difference

between the point of ionisation and the pulse generated by collision of ions with the detector. The velocity of the ions depends on their masses the lighter the ions, the shorter the flight time. TOF can be connected to both a MALDI source and a continuous ion source, such as ESI (Ekman *et al.*, 2009).

1.2.2.2. The Quadrupole mass filter

Quadrupoles are designed to let through only ions in a specified m/z range. They consist of four parallel rods as shown in Figure 1.4. The rods are connected in pairs where they have same potential but with opposite signs. Therefore, ions will experience attractive as well as repulsive forces that that will eventually force them to move towards the middle between the electrodes. Only ions having m/z values within a specified range will have stable trajectories through the quadrupoles, and a given potential ions of lower and higher m/z will collide with rods and never reach the detector (Dass, 2001), varying the potentials allows a range of masses to reach the detector.

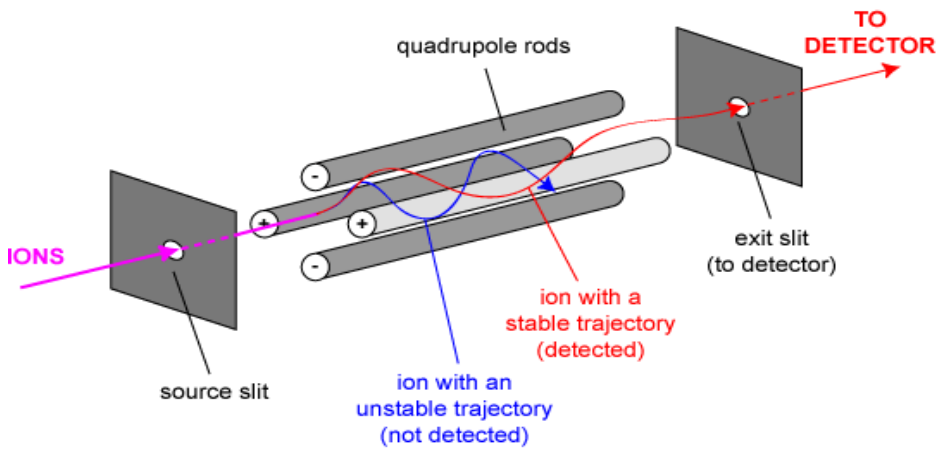

Figure 1.4: Diagram of quadrupole mass analyzer, www.chm.bris.ac.uk/ms/theory/quad-massspec.html.

1.2.2.3. Orbitrap:

The Orbitrap was invented by Makarov. It operates using a central spindle-shaped electrode and outer barrel-like electrode. Ions are trapped around the inner electrode due to the electrostatic field generated between the two electrodes (Qizhi Hu *et al.*, 2005). The electrostatic field urges the ions to move in a spiral pattern because of the balance between the centrifugal force raised from the initial tangential velocity and the electrostatic attraction. Measurement of the m/z value is obtained from the frequency of the harmonic ion oscillations where this frequency is independent of spatial spread of the ions or the energy of the ions themselves (Qizhi Hu *et al.*, 2005). In the LTQ Orbitrap classic the Orbitrap is coupled with and LTQ linear ion trap shown in Figure 1.5.

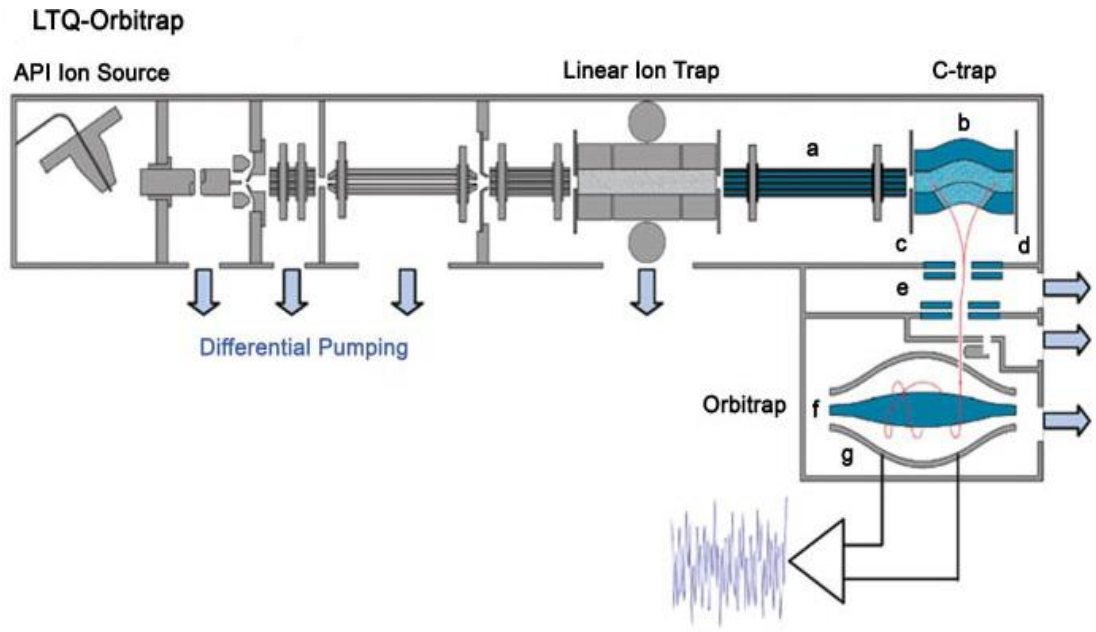

Figure 1.5: Schematics of the commercial LTQ-Orbitrap Classic model (Makarov *et al.*, 2006a): (a) transfer octopole; (b) curved RF-only quadrupole (C-trap); (c) gate electrode; (d) trap electrode; (e) ion optics; (f) inner orbitrap electrode (central electrode);(g) outer orbitrap electrode.

The operation of the LTQ Orbitrap can be briefly described as follows. Ions are transferred from the ion source to the linear ion trap (LTQ) via multipole lenses. Then they are transferred through RF-only octopoles and a gate electrode into the

C-trap. At this stage, the ions are focused by an electrode, a plate at the opposite end of the C-trap. This causes the ions to lose their energy in combination with collisions with N_2 in the trap. Finally, ions are ejected from the C-trap and accelerated towards the Orbitrap in a tight ion beam where they are mass analyzed. The use of the C-trap has minimized the problem of injection of large number of ions into the Orbitrap that might limit its performance as a result of space-charge effects (Makarov *et al.*, 2006; Makarov *et al.*, 2006). The LTQ-Orbitrap is characterized by high mass accuracy (0.5-2 ppm) and high resolving power (up to 150,000). These factors make it useful for analysing complex mixtures. Also it has a relatively low cost, compared to ion cyclotron resonance instruments, which makes it available for many laboratories (Qizhi Hu *et al.*, 2005).

1.3. Ion mobility MS (IMMS):

IMMS utilizes a gas-phase separation mode which separates ions according to their mobility differences in a buffered gas under the effect of a weak electric field (Eiceman *et al.,* 2005). Separating ions according to their size-to-charge ratio which enables the separation of structural isomers that have the same m/z value (Dwivedi *et al*., 2007). IMMS has been used in proteomics although its peak capacity is significantly lower than that of LC or GC.

1.4. Capillary electrophoresis – MS (CE-MS):

CE provides an efficient technique for separating charged metabolites (Ramautar *et al*., 2007; Monton and Soga, 2007). Capillary zone electrophoresis (CZE) is the main CE mode used with MS due to the simplicity of buffer used and lack of a surfactant. Charged molecules are separated according to electrophoretic mobility differences which depend on charge polarity and ionic radius while neutral molecules move through the capillary under electro-osmotic flow (EOF) without separation.

Another advanced mode of CE called MECK, micellar electrokinetic chromatography, in which separation is based on the combination of the

electromobility of the analyte as well as partitioning between the liquid mobile phase and a micellar phase moving at a different rate from the EOF (Bedair and Sumner, 2008). The compatibility of this mode with MS is lower but it does have the ability to separate neutral molecules.

1.5. Gas chromatography mass spectrometry (GC-MS):

GC-MS is one of the most widely used methods in metabolomics (Dettmer *et al.*, 2007; Halket *et al.*, 2005; Kopka, 2006). GC-MS was used in the early 1970s to determine steroids, acids and neutral and acidic drug metabolites in urine (Devaux *et al*., 1971; Horning and Horning, 1970; Horning and Horning, 1971). GC-MS has been utilized for qualitative and quantitative analysis of a wide range of volatile and derivatised non-volatile metabolites. GC-MS is characterized by high analytical reproducibility and lower cost compared to LC-MS and LC-NMR. Generally, GC is coupled with a quadrupole MS or a TOFMS. However, GC-TOF is most popular in metabolomics studies due to higher mass accuracy and mass resolution compared with quadrupoles (Bedair and Sumner, 2008) and because of its greater tolerance of contamination from the derivatising reagents.

The key principle for GC-MS analysis is analyte volatility and thermal stability. However, only small numbers of metabolites are volatile, therefore if possible, the others must be made volatile through chemical derivatisation, which adds complexity and time to an analytical method. Derivatization can be carried out in two steps, firstly, using alkoxyamines to convert the carbonyl groups to oximes which subsequently stabilize the reducing sugars and prevent decarboxylation of α-ketoacids. Secondly, replacement of an active hydrogen with silylation using N-methyl-N-trimethylsilyltrifluoroacetamide (MSTFA) increases thermal stability as well as volatility. However, trimethylsilylation is a water-sensitive process that requires anhydrous conditions. t-butyldimethylsilylation (TBDMS) is less sensitive to water and is usually applied for derivatisation of organic acids and amino acids (Glassop *et al.*, 2007). The drawback of using TBDMS is its high molecular weight

which leads to incomplete derivatisation due to steric hindrance (Halket *et al.*, 2005).

Two dimensional GC (GC×GC) can be used and utilizes two columns with different stationary phase selectivity. This increases resolving power of the technique and enhances the peak capacity of the separation, where TOF-MS is coupled to analyse the data obtained. Multi dimensional GC is also used but it takes time to achieve qualitative and quantitative processing of the complex data obtained (Bedair and Sumner, 2008). GC×GC has been utilized for discovering new metabolic biomarkers for obesity in mice (Shellie *et al*., 2005).

1.6. LC-MS:

LC-MS has been used in numerous metabolomics applications over the past decade (Bajad and Shulaev, 2007; Chen *et al.*, 2007; Dettmer *et al.*, 2007; Wilson *et al.*, 2005). LC-MS can be used for targeted and non-targeted analysis of metabolites. It can help in identifying a larger number of metabolites due to the removal of ionization suppression which takes place in direct infusion mass spectrometry (DIMS). ESI is most commonly coupled with LC. LC provides a low temperature technique which allows analysis of heat labile metabolites. Also, no derivatisation is required prior to LC-MS which in turn saves time and reduces the complexity of the sample preparation procedure. The difficulty of comparing LC-MS data between laboratories is due to the variability of LC-MS systems and the conditions used for the analysis and arises from relative abundances associated with adduct formation, variability of LC retention time indices and variation in fragmentation conditions where MS/MS is carried out (Halket *et al.*, 2005). Therefore, laboratories have had to establish their own libraries for identification of metabolites during their work.

Generally, the most commonly used phases in HPLC analysis are reversed phase C18 or C8 columns where polar metabolites do not show strong retention which may compromise their detection by MS. Retention of polar metabolites can be improved by hydrophilic interaction liquid chromatography (HILIC) (HemstrÖm and

Irgum , 2006) where a water phase is adsorbed onto a stationary phase allowing metabolites to partition between a non-polar mobile phase and a water phase stationary phase (Figure 1.6). Multidimensional LC can also be applied to enhance the separation. 2D-LC/MS comes after 2D-GC/MS in favourability due to the complexity of the experiment and the need for optimising several parameters.

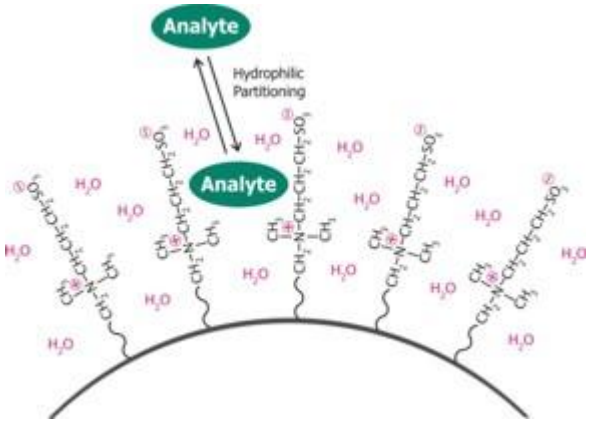

Figure 1.6: Partitioning of the analyte between the mobile phase and the water enriched stationary phase. www.sequant.com/default.asp?ml=11734

The reliability of reversed phase (RP) chromatography for metabolomics has been established as a result of its robustness, reproducibility and well-understood separation mechanism. RP allows the separation of a good range of metabolites. However, due to its limited ability to separate polar metabolites, which are predominant in the aqueous biofluids, other techniques may be required as well. Although normal phase liquid chromatography (NPLC) can separate polar metabolites, its poor reproducibility as well as incompatibility with mass spectrometry systems, in terms of organic eluents such as hexane, have limited its application in metabolomics. As a result, HILIC has become a good alternative for separating polar metabolites (Cubbon *et al.,* 2009).

HILIC can provide good separation for polar metabolites, such as carbohydrates, phosphorylated carbohydrates and glycolytic intermediates, which are particular

poorly retained on a RP column (Dunn and Ellis, 2005). HILIC is similar to NPLC but the non-aqueous mobile phase is replaced by water containing eluent that consists primarily of a water-miscible organic solvent, typically acetonitrile. This consequently allows polar metabolites to interact between water in the mobile phase and water in the stationary phase which in turns provides a good match for MS analysis where the ESI process is favoured by mobile phases with low surface tension. Acetonitrile is preferable over methanol as it provides narrower peaks due to its low viscosity (Bajad *et al.*, 2006). Ammonium formate or acetate (5-20mM) can be used as buffers for HILIC systems because of their solubility in comparatively high organic solvent containing mobile phases. The pH range for HILIC is 3-8 (Guo and Gaiki, 2005).

1.7. Data Processing

Metabolites range in chemical properties from hydrophilic carbohydrates to hydrophobic lipids. The data sets obtained are therefore very complex and need further processing to identify peaks and compounds and interpret the data in terms of biological pathways and statistical significance. Mathematical tools are available to work on reducing the dimensionality of the datasets and to extract significant correlations and biologically meaningful information (Sariyar-Akbulut *et al.*, 2008).

1.7.1. SIMCA P

Discrimination of different groups can be done by principal component analysis (PCA) which is the most commonly used unsupervised chemometrics method. The aim of PCA is to reduce dimensionality of datasets and provide better visualization and analysis of the observations In addition, it reveals relationships between datasets (Cubbon *et al*., 2009).

The first component (PC1), Figure 1.8 accounts for much of the variation in a dataset whereas any subsequent component accounts for smaller amounts of the

remaining variability as the number of the component increases. Therefore, it becomes easier to understand the interaction between groups in a dataset according to their separation by these components and therefore to determine metabolites that are responsible for this discrimination of the populations within the PCA.

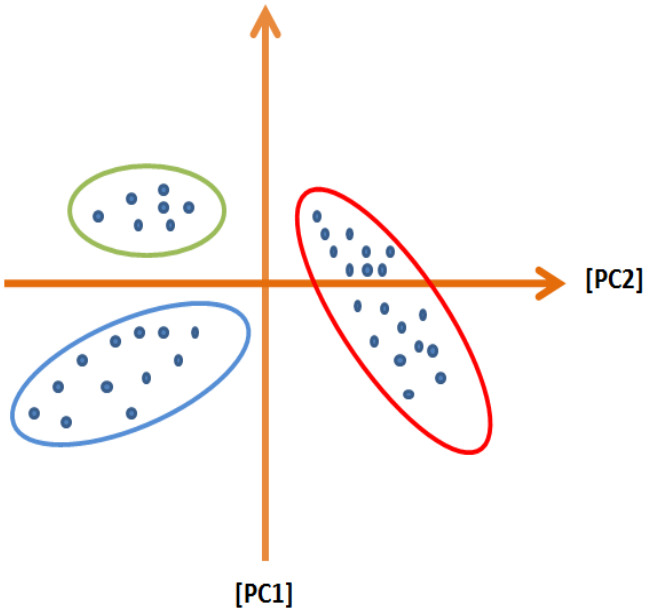

Figure 1.7: An example plot of PCA. PC1 describes the maximum extent of variance between data groups and PC2 accounts for less variance within the dataset.

1.7.2. Sieve software:

In metabolomics, software aims to align chromatograms and extract differences between them, hence, metabolites producing these differences can be determined. There are many types of software available and in the current study the Sieve software provided by ThermoElectron was used in data processing. An example of the output is shown in Figure 1.8, control samples are in red whereas treatment samples in blue. The chromatograms are well aligned and the difference in intensity for a particular extracted ion chromatogram can be easily determined. Sieve software can provide peak intensities for metabolites in addition to their ratio

between control and treatment and p-values. However, p-values are highly dependent on the alignment. If the alignment is not good, then the p-value will not be accurate. Moreover, masses should be checked in the raw data with regard to whether or not they are proper peaks or just background.

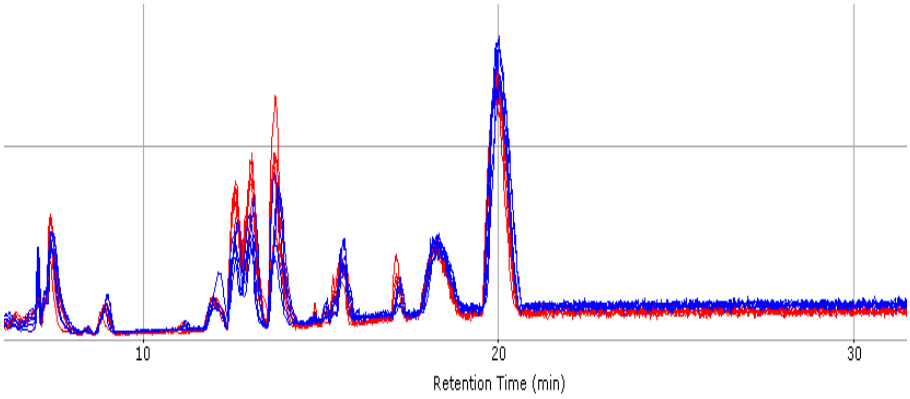

Figure 1.8: Alignment of chromatograms in Sieve.

1.8 Aims and Objectives

The aim of the project was to try to discover more about the glycolytic metabolism of *T.brucei* by using a metabolomic approach in combination with stable isotopic labelling of the metabolome. The glycolytic pathway in trypanosomes is viewed as a potential target for the development of new drugs and a better understanding of it might aid this process. In addition metabolomics was to be used to investigate the mechanism of action of a sample of propolis which had been found to have strong trypanocidal activity.

CHAPTER [2]

GLYCOLYTIC METABOLISM IN *T. BRUCEI*

2.1. Introduction

Trypanosomes are responsible for serious diseases in humans in tropical and subtropical areas. *Trypanosoma brucei* causes sleeping sickness in Africa whereas *Trypanosoma cruzi* is the cause of Chaga's disease in South America. Unfortunately, the available treatment options are neither effective nor safe. Therefore, there is a desperate need to discover new effective treatment strategies (Marie-Astrid Albert *et al*., 2005).

Depending on the host, these parasites use different carbon sources for generating energy. In the blood of a mammalian host, *T. brucei* depends entirely on converting glucose into pyruvate as a source of ATP. In addition, the bloodstream forms (BSF) of trypanosomes have been shown to lack Krebs cycle enzymes and oxidative phosphorylation capabilities. Therefore, glycolysis (Figure 2.1) has become a highly preferred target for designing anti-trypanosomal drugs (Albert *et al*., 2005). However, the insect stage forms, procyclic forms (PCF), depend on L-proline as a carbon source for energy along with at least part of the Krebs cycle (Kamleh *et al*., 2008; Martins *et al.*, 2009; Priest and Hajduk, 1994; Grinsven *et al*., 2009). In BSF, pyruvate is excreted as the only end product of glycolysis whereas in PCF, acetate, succinate and pyruvate are produced when pyruvate is transferred to mitochondria for further oxidation (Wiemer *et al*., 1995; van Grinsven *et al*., 2009).

In blood, trypanosomes appear as long slender trypromastigotes that have poorly developed mitochondria. They can pre adapt for the Tsetse fly midgut environment by transformation into non-dividing short stumpy forms (Queiroz *et al*., 2009; Michels *et al*., 2006). The later have partially developed mitochondria and are capable of producing some proteins that are not found in slender forms (Tyler *et al.*, 1997; Priest and Hajduk, 1994). Density-induced differentiation from BSF into stumpy forms has been reported previously (Vassella *et al*., 1997). Various factors can trigger the transformation of BSF into PCF such as cis-aconitate (Overath *et al*.,

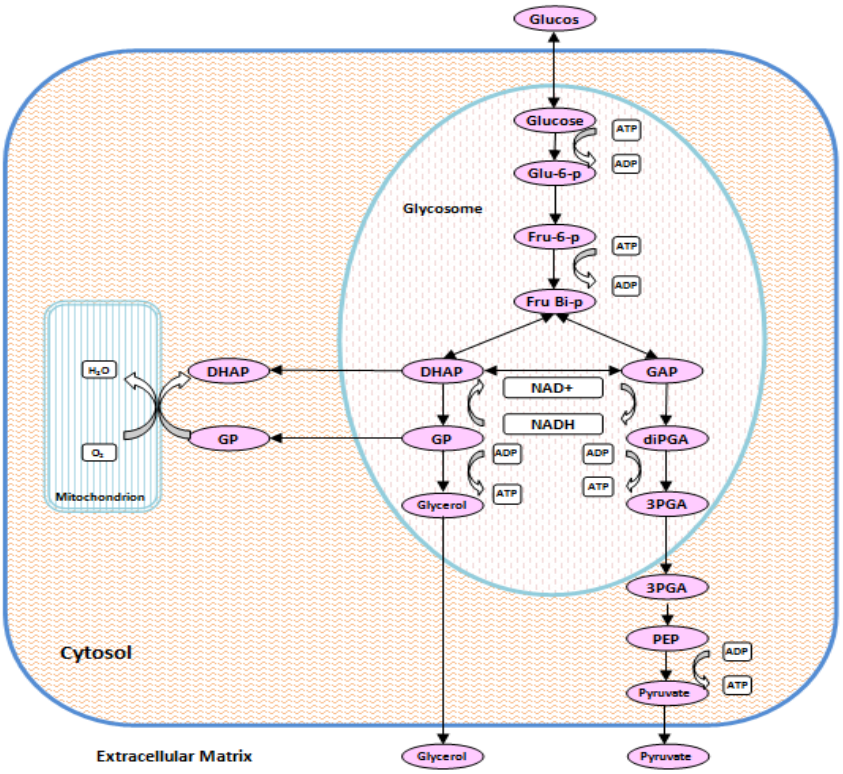

Figure 2.1: Schematic description of glucose metabolism in BSF. Most steps occur in the glycosomes. The mitochondrion is not well developed and pyruvate and glycerol are the main end products of glycolysis. Abbreviations: Glu-6P (glucose-6-phosphate); Fru-6-P (fructose-6-phosphate); Fru Bi-P (fructose bisphosphate); DHAP (dihydroxyacetone phosphate); GP, (glycerol phosphate); GAP (glyceraldehyde-3-phosphate); 1,3-diphosphoglycerate; 3PGA (3-phosphoglycerate); PEP (phosphoenolpyruvate).

1986), acid treatment, proteolytic stress (Rolin *et al*, 1998; Nolan *et al*., 2000) and glucose deprivation (Milne *et al*., 1998).

Recently, an extension of the metabolomics approach, in which labelled metabolic precursors with stable isotopes are used to gain a better understanding of metabolic pathways, has emerged (Zamboni *et al*., 2009; Zamboni and Sauer, 2009). Therefore, growing trypanosomes in a ^{13}C-glucose enriched medium could be a valuable research tool for identifying numerous predicted metabolites in glycolytic pathways. However, identification of some metabolites sets a major challenge in the presence of many possible elemental compositions as well as many possible molecular structures. Therefore, isotopic labelling can be applied as a tool to elucidate a structure of a compound through accurate mass measurement of the labelled metabolite (Giavalisco *et al*., 2008; Hegeman *et al*, 2007). On the other

hand, distinguishing between metabolites of same molecular formula can still be difficult. Hence, strategies for structural elucidation are needed such as comparing chromatographic retention times with standard materials and/or fragmentation patterns.

The aim of the current study was to grow blood stream forms of trypanosomes in a HMI-9 medium which was enriched with $^{13}C_6$-glucose and observe the label incorporation. Then glycolytic intermediates and their labelled counterparts could then be detected using LC-MS and GC-MS. As we were looking at polar metabolites, utilization of HILIC coupled to Orbitrap Fourier transform mass spectrometry (FT-MS) enabled us to elute lipids rapidly and reduce their suppression effect which in addition saves time needed for cleaning column and ESI-MS (Kamleh *et al.*, 2008).

2.2. Materials and Methods

2.2.1 Chemicals:

Water used for HPLC was produced in house using a MilliQ water purification system. HPLC grade acetonitrile was obtained from Fisher Scientific UK, Leicestershire, UK. AnalaR grade formic acid (98%) was obtained from VWR International Limited, Poole, Dorset, UK. U-^{13}C-labelled glucose and N-methyl-N (trimethylsilyl) trifluoroacetamide (MSTFA) were obtained from Sigma Aldrich, Poole, Dorset UK.

2.2.2 Standards:

All biological standards were obtained from Sigma-Aldrich, Dorset UK.

2.2.3 Cell culture and extraction:

$^{13}C_6$-labelled glucose was added to the culture medium in a 4.5g/L concentration in equimolar amount with the unlabelled glucose present in the growth medium. Trypanosomes (Tryp.427 WT) were incubated until they reached about $1.9x10^6$

cell/mL. Cells were separated by centrifugation at 1000rpm at room temperature for 10min. Supernatant was removed as much as possible. Then, cells were washed with FCS-free medium which contained $^{13}C_6$-labelled glucose. Cells were separated by centrifugation at 1000rpm at room temperature for 10 min. Pellets were collected and their volume was made up to 500µL with FCS serum-free medium with $^{13}C_6$-glucose and they were incubated at 37^0C for 30min. They were then split into five portions and centrifuged at 13000rpm at room temperature for 3 min. After centrifugation, supernatant and pellets were added to hot ethanol (80^0C) separately and boiled for 2 min and were then put in ice for 3min. After that, they were centrifuged at 13000rpm for 3min at room temperature. Control cultures were also prepared in a similar manner with using $^{12}C_6$-glucose medium for washing. Samples were stored at -80^0C until they were analysed.

For the 2hr-incubation experiment, cells were grown in $^{12}C_6$-glucose medium then spun down and re-suspended in about 500µL of $^{13}C_6$-glucose-enriched medium and then incubated at 37^0C. Harvesting was carried out at different time points over a 2hr time period.

For the 24 and 48 hr-incubation experiment, cells were grown in $^{13}C_6$-glucose enriched medium and incubated at 37^0C. Harvesting was carried out after 24 and 48hrs.

2.2.4 LC-MS system

The samples were analysed using an LTQ Orbitrap HPLC/MS system (ThermoFisher, Hemel Hempstead, UK). HPLC was carried out using a ThermoFinnigan Surveyor instrument whereas MS was carried out using a ThermoFinnigan LTQ Orbitrap (ThermoFisher, Hemel Hempstead, UK). The analysis was carried out in ESI mode at 4.5 kV using positive and negative ion modes of detection. The mass scanning range was m/z 50-1200, the sheath and auxiliary gas flow rates were 40 and 10 arbitrary units respectively. The capillary temperature was 250 °C. The system was controlled by Xcalibur version 2.0 (ThermoFisher

Corporation). The elution was carried out using a binary gradient mode in which Solvent A was 0.1% v/v formic acid/water; and solvent B was 0.1% v/v formic acid/acetonitrile. The flow rate was 0.3 ml/min. A ZIC-HILIC column (5µm, 150×4.6mm; SeQuant, Darmstadt, Germany) was used for all samples. The linear gradient was: 80% B (0 min) to 50% B at 12 min to 50% B at 26 min to 20% B at 28 min to 20% B at 36min to 80% B at 37min to 80% B at 46min.

For detecting acylated Coenzyme A; the same LTQ orbitrap HPLC/MS system was used, Samples were separated on an AquaSep column (15cmx3.2mm; ES Industries, West Berlin, NJ, USA). The gradient elution system was carried out using solvent A, 95% of 0.1M ammonium formate and 5% Methanol, whereas B solvent system was 50% of 0.1M ammonium formate and 5% methanol. The gradient used was as follows: 100% A (0 min) to 50% A at 20 min to 100%A at 26min (Minkler *et al.*, 2006).

2.2.6 Data Processing

The chromatograms obtained were processed using Sieve version 1.2.0 (Thermo Fisher Scientific Inc., San Jose, USA) and the metabolite id was carried out using an in house macro written in Excel (Sieve, Extractor). PCA was carried out by SIMCA-P version 11.0 (copyright © UMETRICS AB).

2.2.6 GC-MS system

Both samples and reference materials were prepared in the same manner. 200µL of sample was blown to dryness with nitrogen gas. The residue was then silylated with 200µL of MSTFA and allowed to react at 70°C for 30min. Then it was injected into the GC/MS system. Standards were derivatized with MSTFA to give concentrations of 50µg/mL. Analysis was performed with a FOCUS GC and DSQ II single quadrupole MS (ThermoElectron , Hemel Hempstead, UK) operated in electron impact mode. The following conditions were used: 30m × 0.25 mm (i.d) capillary column coated with 100% dimethylpolysiloxane (film thickness, 0.25µm) was used. Temperature was programmed from 80°C (held for 1min) then to 120 °C at 5°C min^{-1} and then

from 120°C up to 320°C at 10°C min^{-1} up to 320°C. Carrier gas (He) pressure was maintained at 87KPa until the end of the run. The injector temperature was 200°C; electron energy, 70eV; source temperature, 200°C; mass range, 50-1020; cycle time, 0.26 s.

2.3. High Density Incubation Labelling studies

2.3.1 Results

LC-MS enabled the accurate detection of a number of metabolites with less than 0.5ppm deviation from their calculated exact mass. The major interest was in metabolites related to energy metabolism in trypanosomes. Unexpected labelling features of glycolytic metabolites were revealed. Standard compounds were run under the same LC/MS conditions where available in order to confirm identity of metabolites in terms of retention times and accurate mass. The instrument was frequently calibrated in order to ensure that masses were usually within 1 ppm of the exact mass of a metabolite. The elements used to carry out elemental matching were restricted to no more than 5 nitrogen atoms, two phosphorus atoms, one sulphur atom, thirty carbon atoms and sixty hydrogen atoms. Since the major interest was in metabolites of <400 amu this generally resulted in only one match within the 1 ppm window. Due to low concentrations of most metabolites, it was difficult to obtain reliable fragmentation patterns. Although samples were concentrated in terms of evaporating the solvent, inconsistent MS/MS patterns were obtained. Succinate was fragmented at 35 V and patterns are shown in appendix VI. On the other hand, the ^{13}C-labelled compounds co-elute with parent molecules in a single LC-MS run which helped in confirming identity of parent compounds.

The design of the metabolomics experiment allowed the detection of glycolytic metabolites in addition to their distribution between extracellular and intracellular compartments. Table 2.1 lists major labelled metabolites detected. Most of the

metabolites identified were shown to have high mass accuracy (<0.5ppm) using either positive or negative modes of detection. Figure 2.2 shows typical total ion chromatograms in positive and negative ion mode for extracts from trypanosome pellets. As pyruvate is well known as the end product of glycolysis, it was detected in high levels. The levels of other metabolites were related to the peak area of pyruvate in order to evaluate how abundant they were. Surprisingly, a number of Krebs cycle metabolites were detected although *T. brucei* was known to lack this cycle (van Hellemond *et al*., 2007). These findings indicated either some Krebs enzymes are functioning in these species or trypanosomes might have been behaving differently as a result of sample handling causing them to change their form.

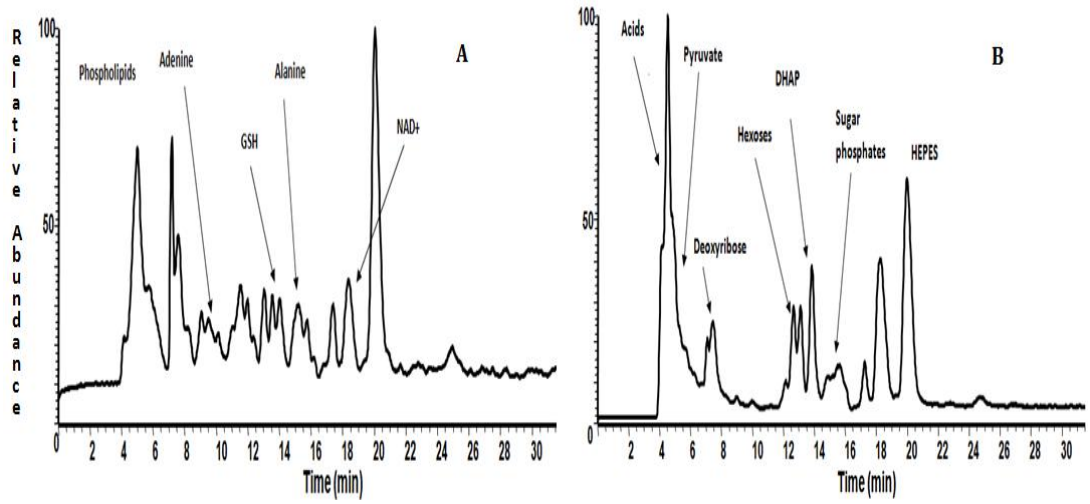

Figure 2.2.: A. TIC for a trypanosome extract on a ZICHILIC column using positive ion mode of detection **B.** TIC for a trypanosome extract on a ZICHILIC column using negative ion mode of detection.

Primarily, files obtained from the LTQ-Orbitrap were processed in Sieve 1.2 and then using an in house Excel based macro Sieve Extractor in order to find possible matches for the masses extracted by Sieve. However, the in-house database was not set to find matches for labelled compounds especially since the labelling patterns could not be fully predicted. Therefore, a PCA model was designed in order to reduce the dimensionality of the data sets (Figure 2.3). PCA was able to find differences between subgroups, labelled and unlabelled pellets and supernatants.

Hence, it was possible to identify which masses contributed to which group and/or subgroup, on that account, prediction of identity of the labelled compounds became easier (Zhang et al, 2009).

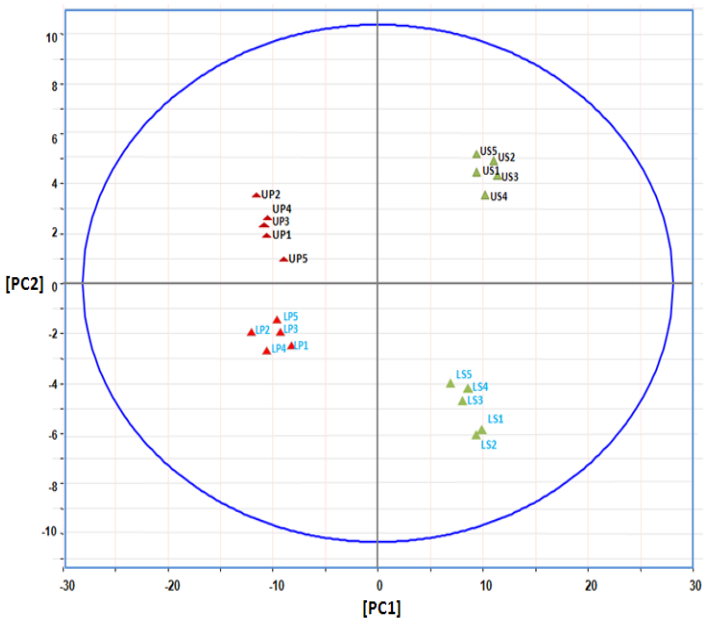

Figure 2.3.: PCA analysis for the datasets obtained using negative ion mode. PC2 separated labelled and unlabeled samples; whereas PC1 identified the differences between pellet and supernatant samples in each group, labelled and unlabelled. Abbreviations: UP: ulabelled pellets; US: unlabelled supernatant; LP: labelled pellets and LS: labelled supernatant.

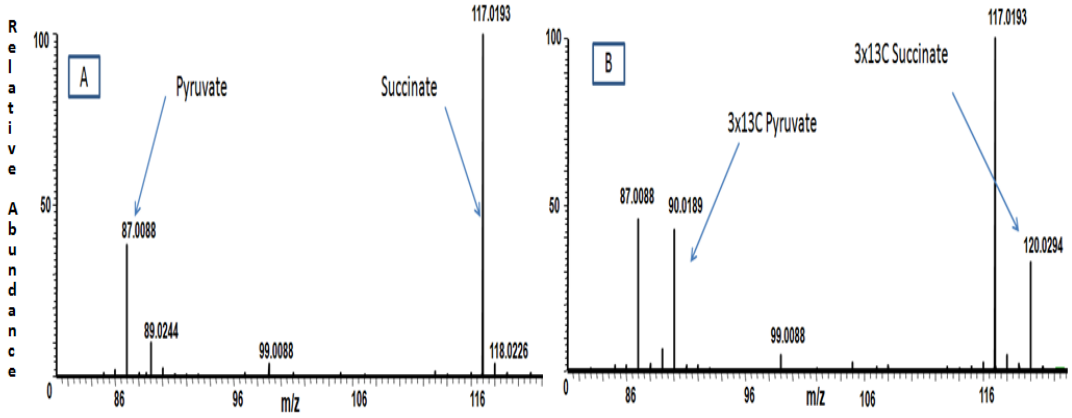

Figure 2.4: A Labelling pattern of succinate and pyruvate from *T. brucei* grown in $^{12}C_6$-glucose. B. Labelling pattern for succinate and pyruvate from *T.brucei* grown in $^{13}C_6$-glucose.

The labelled metabolites were easily detected in the mass spectra since they co-eluted with the corresponding unlabelled compounds. Figure 2.4 shows the labelling patterns for pyruvate and succinate obtained from trypanosomes grown in $^{12}C_6$-glucose and $^{13}C_6$-glucose. Both compounds were labelled with 3 ^{13}C atoms.

When Sieve was used to compare the labelled and un-labelled metabolomes, the labelled metabolites could be picked out easily since they gave clear chromatographic peaks which were absent from the unlabelled samples as shown in Figure 2.5 for selected metabolites. In addition, this experiment allowed relative quantification of these metabolites according to their peak intensities as shown in table 2.1 where the levels of metabolites are compared to the level of the major glycolytic metabolite, pyruvate, and also the level of label incorporation into particular metabolites is compared to the equivalent peak, if any, for the unlabelled metabolite. Finally, the identification was confirmed by running standard compounds for most of the metabolites (Table 2.2). Standards were not available in all cases. As it can be seen from the data in Table 2.1 labelling of the metabolome was more extensive than expected from the previous studies from which it would be predicted that mainly glycolytic intermediates would be labelled.

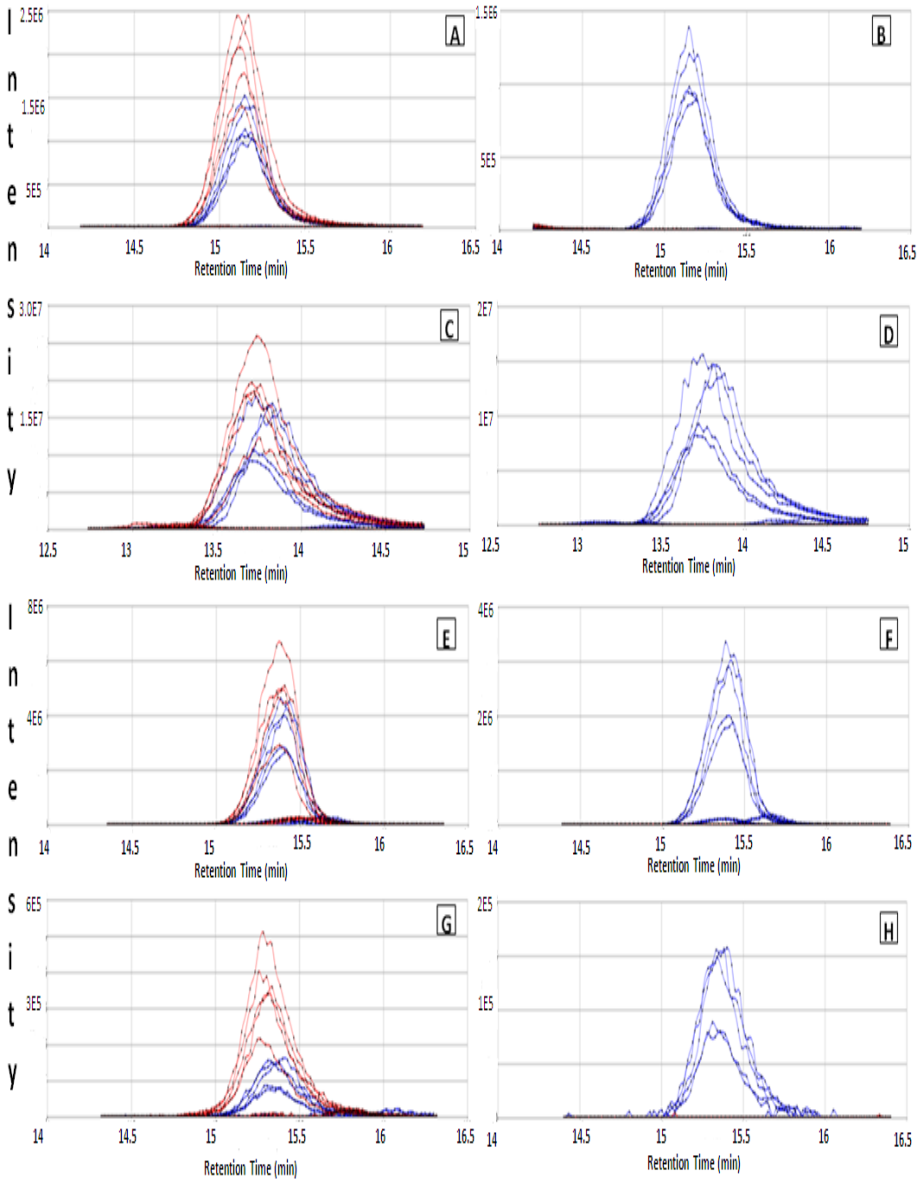

Figure 2.5: Red coloured peaks represent metabolites in ^{12}C-samples. ^{12}C-samples showed higher levels of AMP, glycerol phosphate, glycerophosphoethanolamine and octulose phosphate as shown in A, C, E, and G, respectively. However, their 3x13C-labelled counterparts (shown in blue) were only present in ^{13}C-samples as illustrated by B, D, F and H, respectively.

Table 2.1.: List of labelled metabolites detected. Deviation from the exact mass was <0.1 ppm for most of them. Metabolites with higher ratios were more abundant in cell pellets. These results were obtained from incubation with $^{13}C_6$-glucose at high-cell density

Name	Formula	M-1	RT (min)	Deviation from mass (ppm)	area % relative to 13C pyruvate	% 13C label relative to unlabelled metabolite	area % relative to 13C pyruvate	% 13C label relative to unlabelled metabolite	Distribution: pellets/ supernatant
Glycolysis					pellet		supernatant		
Dihydroxyacetone phosphate	$C_3H_9O_6P$	171.0064	13.8	0.022	718.6	100.0	1.1	100.0	53.0
3x13C Dihydroxyacetone phosphate	$C_3H_9O_6P$	174.0163	13.8	0.018	638.5	88.8	0.9	89.1	52.9
Glucose phosphate	$C_6H_{12}O_9P$	259.0224	14.8	-0.045	33.6	100.0	0.1	100.0	19.8
3 x 13C glucose phosphate	$C_6H_{12}O_9P$	262.0326	14.8	0.091	4.4	13.2	0.0	3.3	78.5
6 x 13 C glucose phosphate	$C_6H_{12}O_9P$	265.0425	14.8	0.111	25.3	75.3	0.0	30.2	49.3
glyceraldehyde phosphate	$C_3H_7O_6P$	168.9908	14.2	0.191	126.9	100	1.6	100	6.6
3x13C glyceraldehydes phosphate	$C_3H_7O_6P$	172.0007	14.2	0.802	126	99.3	1.4	85.5	7.6
Glycerate	$C_3H_6O_4$	105.0193	6.7	0.048	2.7	100.0	3.9	100.0	0.1
3x13C Glycerate	$C_3H_6O_4$	108.0295	6.8	0.004	2.1	77.7	3.6	92.7	0.0
Glycerol	$C_3H_5(OH)_3$	93.0546	9.5	-0.001	0.0	0	40.0	100.0	0.0
3x13C Glycerol	$C_3H_5(OH)_3$	96.06469	9.5	-0.015	0.0	0	39.8	99.4	0.0

Hexoses	$C_6H_{12}O_6$	179.0561	12.4	0.029	75.6	100.0	23.0	100.0	0.3
3 x 13C hexoses	$C_6H_{12}O_6$	182.0662	12.3	0.004	1.0	1.3	0.3	1.5	0.2
6 x 13C hexoses	$C_6H_{12}O_6$	185.0762	12.4	-0.01	72.3	7136.9	21.6	6348.2	0.3
Phosphoenolpyruvate	$C_3H_5O_6P$	166.9751	13.5	0.014	1.5	100.0	0.0	0	only pellet
3x13C phosphoenolpyruvate	$C_3H_5O_6P$	169.9852	13.5	0.024	14.2	960.1	0.0	0	only pellet
Pyruvate	$C_3H_4O_3$	87.00879	6.1	0.031	106.6	100.0	106.2	100.0	0.1
3 x 13C pyruvate	$C_3H_4O_3$	90.01884	6.1	0.008	100.0	93.8	100.0	94.1	0.1
Partially oxidised post-pyruvate metabolites									
Fumarate	$C_4H_4O_4$	115.0037	8.2	0.038	2.0	100.0	0.4	100.0	0.4
3x13C fumarate	$C_4H_4O_4$	118.0138	8.2	0.034	1.2	58.5	0.4	111.5	0.2
Lactic acid	$C_3H_6O_3$	89.02438	7.1	0.013	26.5	100.0	4.7	100.0	0.4
3 x 13 C lactic acid	$C_3H_6O_3$	92.03445	7.1	-0.019	5.7	21.4	1.9	40.1	0.2
Malate	$C_4H_6O_5$	133.0143	8.2	0.053	9.4	100.0	1.8	100.0	0.4
3x13C Malate	$C_4H_6O_5$	136.0243	8.2	0.029	7.4	78.8	1.7	91.5	0.4
Propionic acid	$C_3H_6O_2$	73.02951	6.9	-0.038	31.3	100.0	7.6	100.0	0.3
3 x 13C propionic acid	$C_3H_6O_2$	76.03958	6.9	0.013	5.9	18.8	1.6	20.9	0.3
propionyl phosphate	$C_3H_7O_5P$	152.9959	12.8	0.047	9.5	100.0	0.7	100.0	1.0

3x 13 C propionyl phosphate	$C_3H_7O_5P$	156.0059	12.8	0.053	1.0	10.5	0.4	60.1	0.2
Succinate	$C_4H_6O_4$	117.0194	6.9	0.038	228.4	100.0	85.9	100.0	0.2
3 x 13 C Succinate	$C_4H_6O_4$	120.0294	6.9	0.03	86.1	37.7	36.9	42.9	0.2
Amino acids									
Alanine	$C_3H_7NO_2$	90.05495*	15.1	-0.056	673.0	100.0	47.5	100.0	1.1
3x13C Alanine	$C_3H_7NO_2$	93.065*	15.1	0.006	734.3	109.1	48.7	102.5	1.2
N-acetyl lysine	$C_8H_{16}O_3N_2$	187.1088	13.3	0.014	0.0	100.0	2.2	100.0	0.0
2 x 13C labelled N-acetyl lysine	$C_6C_2H_{16}O_3N_2$	189.1155	13.3	-0.005	3.1	10536.0	0.5	24.1	0.4
Ascorbate pathway									
Glucuronic acid	$C_6H_{10}O_7$	193.0354	5.8	0.014	0.0	100.0	0.3	100.0	0.0
3xC13 glucuronic acid	$C_6H_{10}O_7$	196.0452	5.3	0.06	0.0	0.0	0.5	153.3	0.0
6xC13 glucuronic acid	$C_6H_{10}O_7$	199.0549	6.0	-0.035	0.0	0.0	0.3	0.0	0.0
Pentose phosphate pathway									
Deoxyribose	$C_5H_{10}O_4$	133.0507	7.1	0.028	16.8	100.0	0.9	100.0	1.5
2 x 13C deoxyribose	$C_5H_{10}O_4$	135.0574	7.1	0.018	11.6	68.9	0.5	52.3	1.9
3 x 13 C deoxyribose	$C_5H_{10}O_4$	136.0608	7.1	0.014	12.3	73.5	0.6	62.2	1.7
5 x 13 C deoxyribose	$C_5H_{10}O_4$	138.0674	7.1	-0.026	8.4	50.1	0.3	34.6	2.1

gluconic acid	$C_6H_{12}O_7$	195.051	13.5	-0.016	7.2	100.0	0.7	100.0	0.8
3 x 13C gluconic acid	$C_6H_{12}O_7$	198.0611	13.5	-0.09	36.7	560.7	0.6	165.3	4.6
6 x 13C gluconic acid	$C_6H_{12}O_7$	201.0711	13.5	-0.015	6.6	90.6	0.4	55.7	1.4
Ribose	$C_5H_{10}O_5$	149.0456	9.9	0.043	6.7	100.0	2.8	100.0	0.2
2 x 13C ribose	$C_5H_{10}O_5$	151.0523	10.0	-0.006	1.2	17.3	0.3	12.3	0.3
3 x 13C ribose	$C_5H_{10}O_5$	152.0557	9.9	0.049	1.2	18.3	0.3	12.3	0.3
4 x 13C ribose	$C_5H_{10}O_5$	153.0592	10.0	-0.066	0.0	0.0	0.1	3.5	0.0
5 x 13C ribose	$C_5H_{10}O_5$	154.0623	9.9	0.009	6.0	89.5	2.2	78.2	0.2
ribose phosphate	$C_5H_{11}O_8P$	229.0118	14.2	-0.031	9.9	100.0	0.0	100.0	23.8
5 x 13 C ribose phosphate	$C_5H_{11}O_8P$	234.0287	14.1	-0.175	8.9	89.9	0.0	83.8	25.6
7 C sugars	$C_7H_{13}O_8$	225.0614	12.4	-0.091	86.0	100.0	25.7	100.0	0.3
6 x C13 - 7C sugars	$C_7H_{13}O_8$	231.0815	12.4	-0.084	86.5	100.6	25.8	100.5	0.3
sedoheptulose phosphate	$C_7H_{15}O_{10}P$	289.033	15.1	-0.056	0.8	100.0	0.0	0.0	only pellet
3x13C sedoheptulose phosphate	$C_7H_{15}O_{10}P$	292.0431	15.1	0.066	0.4	49.9	0.0	0.0	only pellet
7x13C sedoheptulose phosphate	$C_7H_{15}O_{10}P$	296.0565	15.0	0.203	0.4	45.8	0.0	0.0	only pellet
unknown C9 sugar phosphate	$C_9H_{14}O_{10}P$	312.0255	15.4	-0.131	4.5	100.0	0.0	only pellet	2214.3
3 x 13C unknown C9sugar phosphate	$C_9H_{14}O_{10}P$	315.0356	15.4	0.244	3.1	69.6	0.0	only pellet	1299.0

unknown C9 sugar phosphate	$C_9H_{19}O_{11}P$	333.0591	14.9	-0.021	9.4	100.0	0.4	100.0	1.8
3 x 13Cunknown C9 sugar phosphate	$C_9H_{19}O_{11}P$	336.069	14.9	-0.105	5.9	63.3	0.2	57.9	2.0
6 x 13C unknown C9 sugar phosphate	$C_9H_{19}O_{11}P$	339.0793	14.9	0.06	8.9	94.3	0.1	25.8	6.6
9 x 13 C unknown C9 sugar phosphate	$C_9H_{19}O_{11}P$	342.0894	14.9	-0.024	5.5	58.7	only pellet	only pellet	only pellet
unknown C9 sugar phosphate	$C_9H_{18}O_{12}P$	349.0541	15.6	0.098	1.7	100.0	0.0	100.0	183.8
3 x 13Cunknown C9 sugar phosphate	$C_9H_{18}O_{12}P$	352.06415	15.7	0.199	1.7	99.1	0.0	only pellet	459.0
6 x 13C unknown C9 sugar phosphate	$C_9H_{18}O_{12}P$	355.07452	15.7	0.128	1.7	102.9	0.0	only pellet	only pellet
9 x 13 C unknown C9 sugar phosphate	$C_9H_{18}O_{12}P$	358.0841	15.5	0.31	4.4	256.8	0.0	only pellet	only pellet
unknown C8 sugar phosphate	$C_8H_{17}O_{11}P$	319.0435	15.4	-0.051	4.8	100.0	0.0	100.0	9.8
3 x13C unknown C8 sugar phosphate	$C_8H_{17}O_{11}P$	322.0536	15.4	-0.015	4.8	100.8	0.0	2.5	395.0
5 x 13C unknown C8 sugar phosphate	$C_8H_{17}O_{11}P$	324.0604	15.4	0.015	4.5	94.8	0.0	122.6	7.6
8 x 13C unknown C8 sugar phosphate	$C_8H_{17}O_{11}P$	327.0705	15.4	0.021	4.0	83.2	0.0	0.0	552.1
Nucleotides									
Adenosine	$C_{10}H_{13}N_5O_4$	268.1042*	11.8	0.11	15.9	100.0	0.0	100.0	196.8
5x13C Adenosine	$C_{10}H_{13}N_5O_4$	273.121*	11.8	0.041	14.2	89.0	0.0	88.6	197.7
AMP	$C_{10}H_{14}O_7N_5P$	346.0558	15.2	-0.017	43.4	100.0	0.0	100.0	224.3
5 x 13C AMP	$C_{10}H_{14}O_7N_5P$	351.0725	15.2	-0.101	38.2	88.1	0.0	107.2	184.3

5'-Methylthioadenosine	$C_{11}H_{15}N_5O_3S$	298.097*	9.4	-0.022	156.8	100.0	1.7	100.0	7.0
5x13C 5'-Methylthioadenosine	$C_{11}H_{15}N_5O_3S$	303.1135*	9.4	-1.281	130.4	83.2	1.4	81.8	7.1
NAD+	$C_{21}H_{27}N_7O_{14}P_2$	664.1162*	16.7	0.184	12.7	100.0	0.0	100.0	only pellet
5x13C NAD+	$C_{21}H_{27}N_7O_{14}P_2$	669.133*	16.8	0.102	24.8	195.5	0.0	only pellet	only pellet
Uracil	$C_4H_4N_2O_2$	113.0345*	7.8	-0.035	3.3	100.0	4.3	100.0	0.1
2x13C Uracil	$C_4H_4N_2O_2$	115.0412*	7.6	-1.335	1.2	36.4	2.3	54.4	0.0
Uridine	$C_9H_{12}N_2O_6$	243.0623	10.5	0.044	2.5	100.0	0.1	100.0	1.8
2 x 13C uridine	$C_9H_{12}N_2O_6$	245.069	10.5	-0.077	1.6	63.0	0.1	126.9	0.9
uridine x 5 13C	$C_9H_{12}N_2O_6$	248.079	10.5	-0.094	3.3	134.7	0.8	715.8	0.3
uridine x 7 13C	$C_9H_{12}N_2O_6$	250.0858	10.5	-0.012	1.2	46.4	0.0	25.4	3.2
Glycerolipids									
diglycerol phos	C6 H15O8 P	245.0431	12.604	0.134	1083.2	100.0	1.3	100.0	68.4
3 x 13C diglycerol phosphate	C6 H15 O8 P	248.0532	12.6	-0.127	1702.0	157.1	0.9	65.4	164.3
6 x 13C diglycerol phosphate	C6 H15 O8 P	251.0632	12.6	-0.302	618.4	57.1	0.0	0.0	only pellet
glycerophosphoethanolamine	$C_5H_{14}O_6NP$	214.0486	15.4	-0.017	120.2	100.0	0.5	100.0	19.4
3 x13 C glycerophosphoethanolamine	$C_5H_{14}O_6NP$	217.0585	15.4	-0.017	84.5	70.4	0.3	66.0	20.7
Glycoconjugate sysnthesis									

glucosamine phosphate	$C_6H_{14}O_8NP$	258.0384	15.0	-0.024	12.4	100.0	0.1	100.0	17.0
3 x 13C glucosamine phosphate	$C_6H_{14}O_8NP$	261.0484	15.0	-0.002	7.6	61.5	0.0	64.1	16.3
N-acetylglucosamine phosphate	$C_8H_{15}O_9NP$	300.049	13.6	0.064	14.0	100.0	0.0	100.0	81.0
2 x 13C N-acetylglucosamine phosphate	$C_8H_{15}O_9NP$	302.0558	13.6	-0.134	2.9	20.6	0.0	218.8	7.6
3x 13C N-acetylglucosamine phosphate	$C_8H_{15}O_9NP$	303.0591	13.6	0.181	2.3	16.2	0.0	15.4	85.1
6 x 13 C N-acetylglucosamine phosphate	$C_8H_{15}O_9NP$	306.0693	13.5	-0.097	14.1	100.6	0.0	23.8	342.7
8 x 13C N-acetylglucosamine phosphate	$C_8H_{15}O_9NP$	308.0759	13.5	0.133	3.0	21.1	0.0	116.4	14.7

*These masses represent M+1 where they were detected on positive ion mode.

2.3.2 High Density Labelling Studies Discussion:

During the course of this study, it was noticed that both sample preparation protocols and extraction solvents might cause the results to vary significantly. Consequently, different extraction protocols were followed in order to reduce any chance of the trypanosomes to change their metabolism as a response to the surrounding environment. For instance, diluted cultures were analysed to exclude the effect of crowding and nutrition depletion. In addition, a minimal handling procedure was carried out which involved centrifuging the cells once before quenching them into hot ethanol thus avoiding washing steps and unnecessary stress. Furthermore, acetonitrile was used as a final extraction solvent to eliminate any effect that alcohol, namely ethanol, might have in generating artefacts from the biologically produced metabolites.

From the biological point of view, many of the observed metabolites were known before. Nevertheless, some interesting findings indicated that there were some biological questions to be answered. As mentioned before, bloodstream forms were reported to be lacking the Kreb's cycle and hence the metabolites produced from it. Yet, some of these metabolites were found in the samples studied along with their labelled correlates. Accordingly, the challenge of trying to identify these metabolites and prove that they were not an artefact of handling procedures was taken up.

According to the conditions of the experiment, cells were incubated at high density (9.5×10^{8} cell/ml) in a very small volume in an attempt to get a concentrated pool of labelled metabolites. Consequently, cells would be highly depleted of glucose which in turn could trigger the transformation into PCF. Additionally, as almost all acids were excreted, pH of the culture medium would be significantly reduced which again could contribute to triggering the transformation into PCF. In addition there was an interest in the production of a possibly quorum

sensing factor responsible for promoting the transformation of BSF into stumpy forms-the stumpy induction factor.

2.3.2.1 Glycolytic metabolites

Clear labelling of the glycolytic intermediates hexose phosphate, glyceraldehyde phosphate, dihydroxyacetone phosphate, glyceric acid, phosphoenol pyruvate and pyruvate can be observed (Table 2.1). This pattern of labelling is in line with what would be predicted for BSF with all the metabolites being 3 or 6 carbon labelled. Glycolytic intermediates were retained mainly inside the cells except for hexoses and pyruvate. The high levels of production of pyruvate reflect those observed previously for normal glycolysis in BSF whereas in PSF it would be utilized for production of acetate, alanine, ethanol and lactate (Weimer *et al.*, 1995; Bringaud *et al.*, 2006; van Grinsven *et al.*, 2009). In addition, secretion of pyruvate into the medium indicates that no further metabolism is converting it into acetyl-CoA as it would have to be retained inside cells for this to occur rather than being secreted. This is one deviation for the expected pattern in glycoloytic metabolites. Another is the presence of a small amount of $^{13}C_3$ hexose which indicated that gluconeogensis might be happening in these cultures, alternatively the glycolytic pathway might be reversible with the trioses being recombined to make glucose. Neither of these pathways have been previously reported as a pathway in trypanosomes.

2.3.2.2 Partially oxidized post pyruvate metabolites

The Krebs cycle has not been reported to be present in BSF before. The metabolites within the Krebs cycle which became labelled include succinate and fumarate. The succinate levels in the pellet were almost as high as those of pyruvate, assuming a similar response factor (Table 2.1) and thus it was a significant rather than a trace metabolite. At first sight it might be assumed that the Krebs cycle was producing succinic acid but the succinic in the incubations is $^{13}C_3$-labelled and thus cannot come from incorporation of acetate which occurs in the Krebs cycle

which only produces $^{13}C_2$-labelled metabolites or eventually $^{13}C_4$-labelled metabolites if enough time is allowed for complete labelling of the metabolome. Other possibilities for succinate biosynthesis are via the propionate pathway or via phosphoenol pyruvate, oxaloacetate, fumarate and finally succinate (Appendix III and Appendix V). Both these pathways would produce $^{13}C_3$-labelled metabolites. Appendix VI shows the MS^2 spectrum for $^{13}C_3$-labelled and unlabelled succinate, the ions at m/z 102 and m/z 99 indicate loss of water from the labelled and unlabelled metabolites respectively. In the case of the $^{13}C_3$-labelled the ions at m/z 75 and 76 indicate loss of CO_2 from the molecular ion indicating that, as might be expected, one of the COOH groups in the molecule is labelled. The propionate pathway does seem to be very active within the trypanosomes since high levels of label incorporation in lactic acid, propionic acid and propionyl phosphate can be observed. Van Grinsven *et al* mentioned in their experiments that incubation of long slender forms of BSF in mice for 7 days led to 92% of cells being transformed into short stumpy forms which accounted for the presence of postpyruvate metabolites as the stumpy form of trypanosomes have a functioning mitochondrion (van Grinsven *et al*., 2009). In Leishmania and other trypanosomatids, the generation of succinate might be used for maintaining balance of NAD+/NADH because of their depletion during glycolysis. Therefore, conversion of PEP into succinate will generate two NAD+ molecules as well as malate and fumarate as intermediates (Saunders *et al*., 2009; Bringaud *et al.*, 2006). Further labelling experiments will be required in order to elucidate this pathway.

2.3.2.3 Aminoacids

High levels of alanine in the culture suggest that there are functioning alanine aminotransferases, which is not expected in BSF, whereas alanine is the main end product of proline metabolism in PCF (Marr and Muller, 1995; Spitzangel *et al*., 2009). The alanine produced in this study was $^{13}C_3$- labelled suggesting that it was produced from pyruvate. Previous studies have suggested that increased levels of alanine might reflect depletion of glucose which might be true under the conditions

of our experiment (Coustou *et al*., 2008). In addition, alanine might be produced as a mechanism of excreting ammonia or as an osmosis-stabilizing metabolite (Marr and Muller, 1995). However, formation of alanine needs an amino group donor, another amino acid. In the current experiment there was a significant increase of α-ketoglutarate in the FCS free growth medium which does not contain this metabolite suggesting that glutamate might function as the amino group donor.

Most of the amino acids in the pellets apart from alanine were not labelled, however, N-acetyl lysine was present as $^{13}C_2$-N-acetyl lysine suggesting that lysine was acetylated with $^{13}C_2$-acetyl CoA as an acetyl-moiety donor, however, it is possible that acetylation can be carried out via acetyl phosphate. However, acetyl CoA was not detected by the LC-MS system although 3-hydroxybutyrate was detected which is thought to be a by-product of acetyl CoA metabolism (Coustou *et al*., 2008). Sowers and colleagues reported that N-acetyl lysine was produced in some species of bacteria and eucarya as osmoregulatory metabolite (Sowers and Gunsalus, 1995). However, in the current study its levels were found to be higher in the extracellular compartment.

2.3.2.4 Ascorbate pathway

At the first sight it was thought that there were high levels of ascorbate in the supernatant with its $^{13}C_3$ and $^{13}C_6$ labelled counterparts. In fact, initially it was thought that ascorbate might be a candidate for stumpy induction factor. However, fragmentation pattern of the "ascorbate" in the samples, Figure 2.6 , was different from that of the ascorbate standard and also from that obtained for isoascorbic acid-and the chromatographic retention time of the unknown material was earlier than that of ascorbate. It is possible that this isomer of ascorbate might be generated from dimerization of pyruvate to form parapyruvate. Pyruvate is produced in high levels in the growth medium and the possibility of parapyruvate forming from pyruvate was suggested previously (Miyata and Yonehara, 1996). Moreover, this dimerization was also seen in a solution of concentrated pyruvate standard material injected into the mass spectrometer, Figure 2.7 producing a

dimer peak isomeric with the at a later time than the main pyruvate peak. It is not clear whether this dimer is present in the pyruvate standard, is formed on column or is formed in a concentration dependent manner in the mass spectrometer.

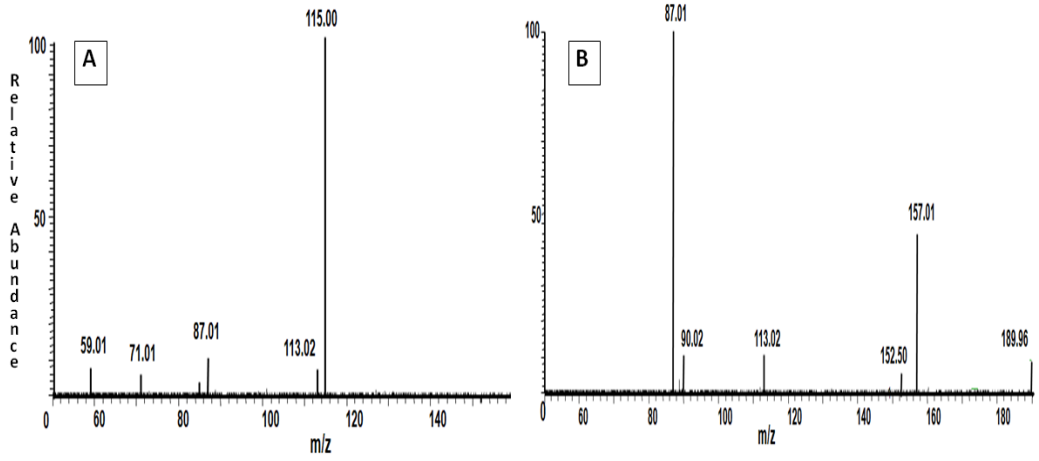

Figure 2.6.: A, MS^2 fragmentation patterns of ascorbate standard material which does not match that of the isomeric peak found in the samples, **B,** CID voltage was 30V.

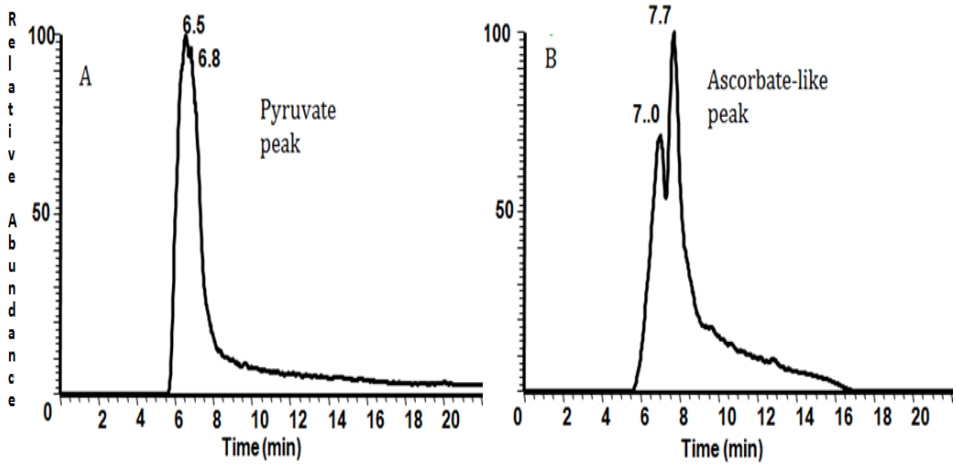

Figure 2.7: A, represents the peak of pyruvate obtained from a concentrated standard solution whereas in B, m/z 175.02 was found later than pyruvate in the same standard solution.

2.3.2.5 Pentose phosphate pathway

The pentose phosphate pathway was functioning efficiently in the cultures under high density incubation. Surprisingly, nonulose phosphate and octulose phosphate, which have certainly not been described before in trypanosomes or indeed anywhere in the case of nonulose phosphate, were detected. These polyols may be synthesised to sustain osmosis inside cells and thus reduce water loss into

the surrounding medium (Strange, 2004; Davis *et al.*, 2000). Heptulose phosphate, on the other hand was mainly excreted and was present only in small amounts. The labelling patterns of the octulose and nonulose phosphates were complex but basically suggested combination of 3-carbon units with pentose or hexose. The complex labelling pattern of octulose phosphate is shown in Figure 2.8 and indicates that the molecule is composed of a 5x ^{13}C carbon units and a 3 x ^{13}C carbon unit. This suggests that octulose phosphate is being formed from fructose phosphate in combination with a 5 carbon molecule such as xylose phosphate in the same way as the more commonly observed heptulose phosphate is formed from fructose phosphate and erythrose phosphate. Three carbons are derived from fructose phosphate and five are derived from erythrose phosphate giving a 0, 3, 5, 8 pattern. This indicates that transketolase in trypanosomes is able to accept a variety of substrates. Small amounts of nonulose phosphate are observed in the extracts and this has a 3x ^{13}C, 6 x ^{13}C , 9 x ^{13}C labelling pattern indicating that it is probably formed from two fructose phosphate molecules.

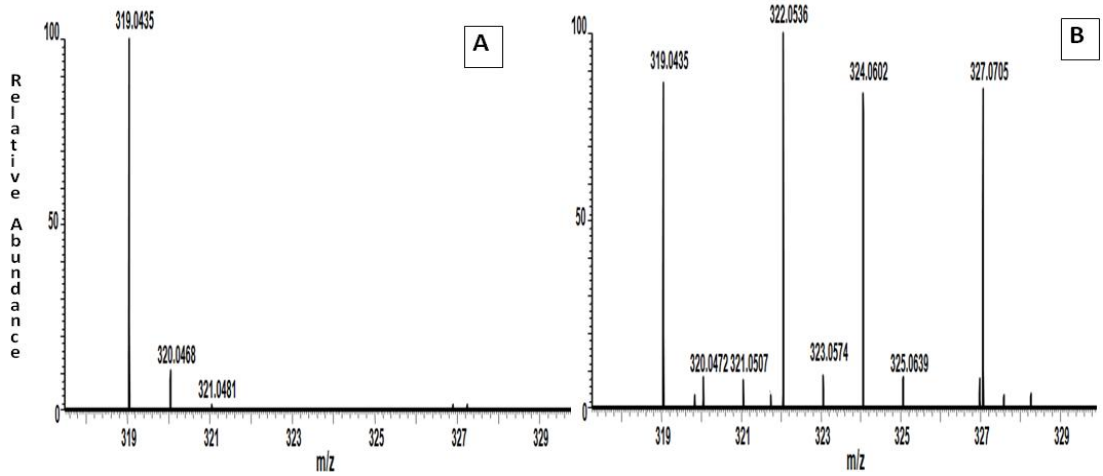

Figure 2.8: A, Octulose phosphate in U^{12}C-glucose samples in comparison with labelling patterns that can be easily seen in trypanosomes incubated with U ^{13}C-glucose in **B**.

Other molecules in the pentose phosphate pathway including deoxyribose, ribose and ribose/xylulose phosphate (these appeared as two isomeric peaksbut have not

been distinguished). The presence of $^{13}C_5$-ribose and ribose phosphate led to the labelling of nucleotides, for example adenosine and AMP were both $^{13}C_5$-labelled.

2.3.2.6 Nucleotides

Nucleotides were mainly concentrated inside the cells. $^{13}C_5$-moities in uridine may be from $^{13}C_5$-ribose. However, the $^{13}C_7$-uridine observed has to be due to $^{13}C_5$-ribose plus $^{13}C_2$-uracil and thus suggests that uracil is synthesised from a labelled beta-alanine precursor. There was no evidence of labelled beta-alanine in the cells, although initially it was thought to be labelled beta-alanine which was present in the growth medium but this appeared to be an artefact produced by residual salts in the medium sample causing peak splitting on the ZICHILIC column. Adenosine, AMP, methylthioadenosine and NAD+ were all labelled with $^{13}C_5$-ribose.

2.3.2.7 Glycerolipids

The glycerolipids were not excreted into the growth medium. The $^{13}C_3$-labelled pattern for the glycerol phospholipids may be accounted for by the incorporation of $^{13}C_3$-glycerol. High levels of labelled $^{13}C_3$-glycerol phosphate, $^{13}C_3$-phosphoethanolamine and $^{13}C_3$-glycerophosphatidyl choline could be observed in the cell pellets.

2.3.2.8 Glucoconjugates

^{13}C-label was incorporated in different patterns in N-acetylglucosamine phosphate, glucosamine phosphate was only $^{13}C_3$-labelled. Both of them were retained within the cells. The identity of most of the metabolites was checked with standard materials run under the same chromatographic conditions and masses obtained are shown in the table below (Table 2.2). As can be seen some of the isomeric compounds run closely and thus identity in these cases can only be putative.

Table2.2: List of standard materials and their retention times on ZicHILIC that helped in identifying some metabolites related to the Krebs cycle, glycolysis and pentose phosphate pathway.

No.	Name	Formula	mass	Retention time(min)	Deviation (ppm)
1.	α-ketoglutaric acid	$C_5H_6O_5$	145.01428	8.16	0.229
2.	Ascorbate	$C_6H_8O_6$	175.02480	10.59	-0.06
3.	Dihydroxy acetone phosphate	$C_3H_7O_6P$	168.99083	14.94	0.47
4.	Erythrose-4-phosphate	$C_4H_9O_7P$	199.00151	16.12	0.982
5.	Fructose-1-phosphate	$C_6H_{13}O_9P$	259.02234	15.88	-0.4
6.	Fructose-6-phosphate	$C_6H_{13}O_9P$	259.02234	16.05	-0.4
7.	Fumarate	$C_4H_4O_4$	115.00368	6.25	-0.018
8.	Galactose-6-phosphate	$C_6H_{13}O_9P$	259.02243	16.13	-0.054
9.	Gluconic acid	$C_6H_{12}O_7$	195.05139	14.04	1.8
10.	Glucose-6-phosphate	$C_6H_{13}O_9P$	259.02274	15.77	1.14
11.	Glyceraldehyde phosphate	$C_3H_7O_6P$	168.99088	16.34	0.77
12.	Lactate	$C_3H_6O_3$	89.02450	6.48	0.814
13.	Methylmalonic acid	$C_4H_6O_4$	117.01929	6.51	-0.36
14.	N-acetyl lysine	$C_8H_{16}O_3N_2$	187.10884	13.88	0.13
15.	N-acetylglucosamine phosphate	$C_8H_{16}O_9NP$	300.04904	15.21	0.16
16.	Pyruvate	$C_3H_4O_3$	87.00875	6.54	-0.2
17.	Ribose-1-phosphate	$C_5H_{11}O_8P$	229.01195	14.99	0.31
18.	Ribose-5-phosphate	$C_5H_{11}O_8P$	229.01196	15.76	0.35
19.	Succinate	$C_4H_6O_4$	117.0193	6.35	0.238

2.4 Labelling studies with $^{13}C_6$-glucose over 2 hours

2.4.1 Results

Incubation of trypanosomes at high density, as in the previous experiment, was carried out in order to follow the accumulation of metabolites over time in addition to following the incorporation of labelling. $^{13}C_6$-glucose was added immediately before the incubation step and prior to this point cultivation was in ^{12}C-glucose. Following addition of $^{13}C_6$-glucose harvesting was carried out at different time points. Figure 2.9 shows plots of metabolite accumulation with time from the point where the cultures were transferred into a high density culture and Figure 2.10 shows the incorporation of label with time. The % label incorporation and the number of compounds labelled were lower in this experiment in comparison with where the cultures were grown in $^{13}C_6$-glucose from the outset.

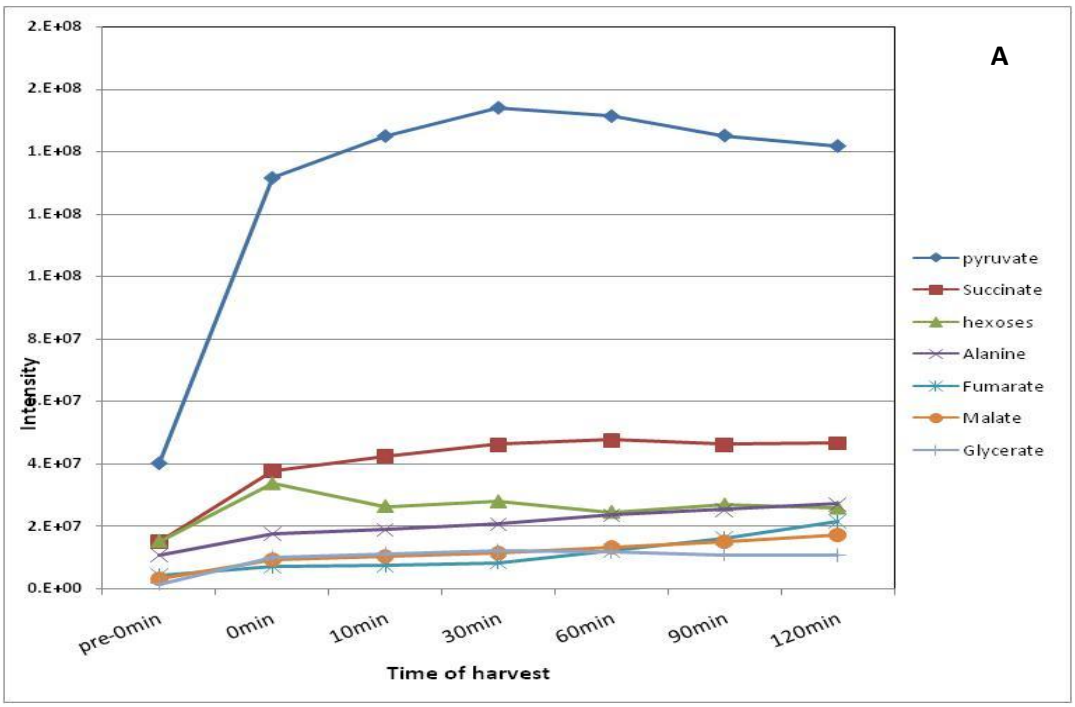

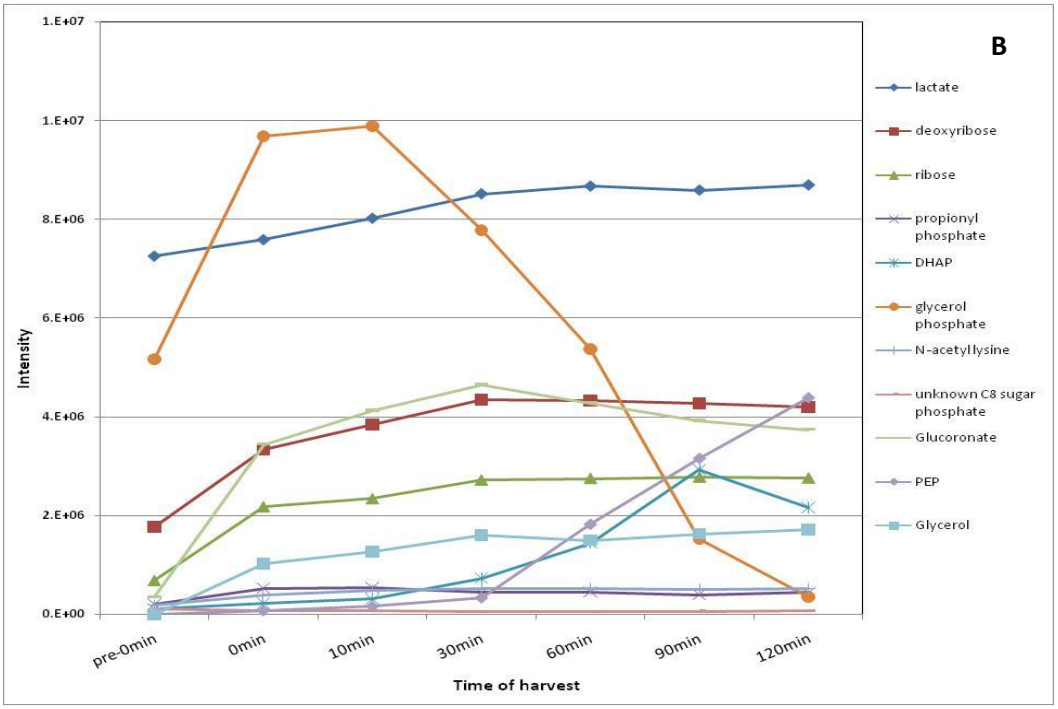

Figure 2.9.: A, **B** represent the accumulation of some major metabolites over two-hour incubation at high cell density as judged by peak area for each metabolite obtained in the mass spectrometer. The values plotted represent total sums of labelled and un-labelled species for each metabolite.

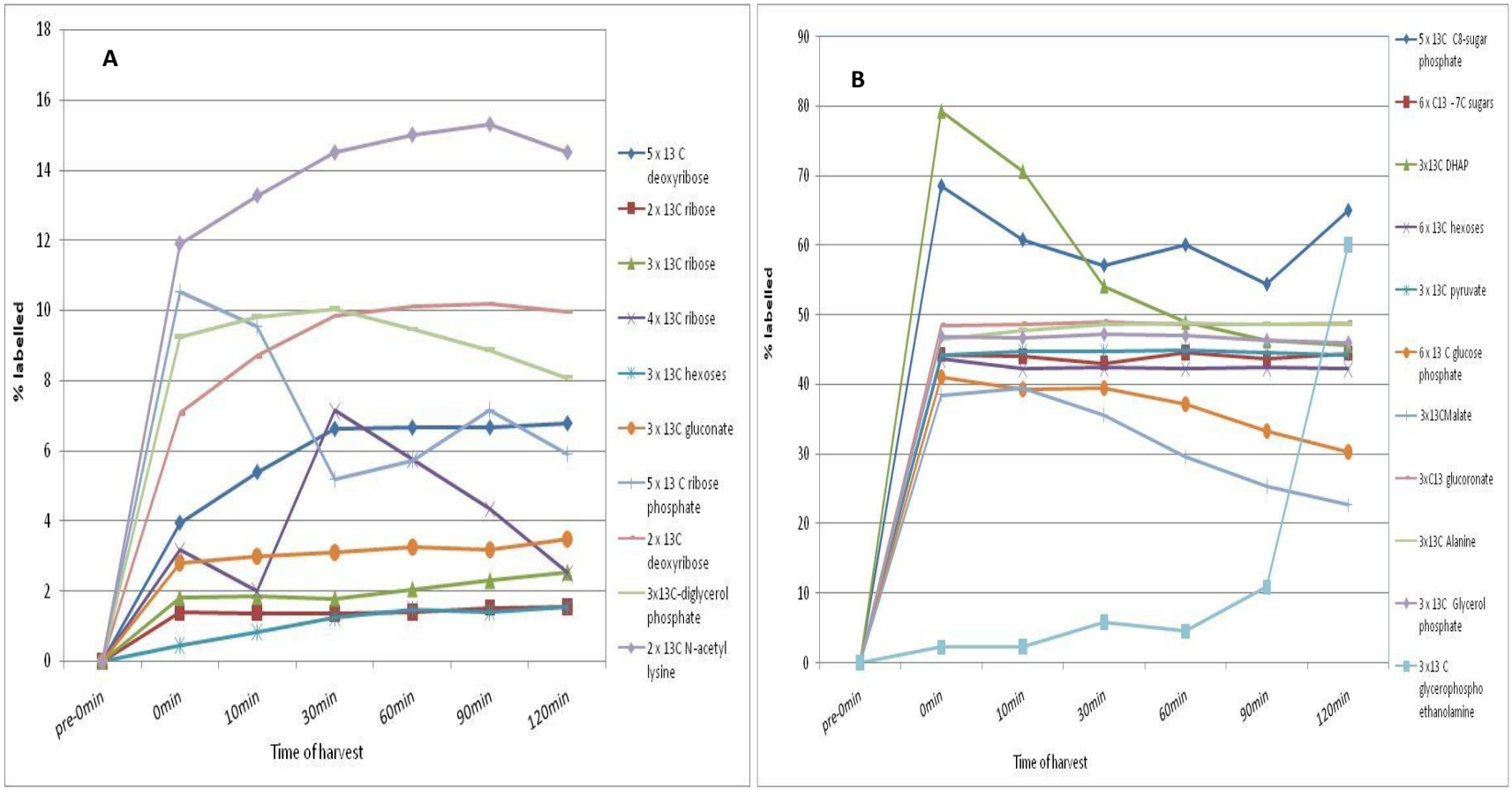

Figure 2.10: A and B show levels of metabolites from cultures incubated with $^{13}C_6$-glucose and samples were collected at different time points. Generally levels started to level off after 60min. At pre-0min, samples before incubation with $^{13}C_6$-glucose.

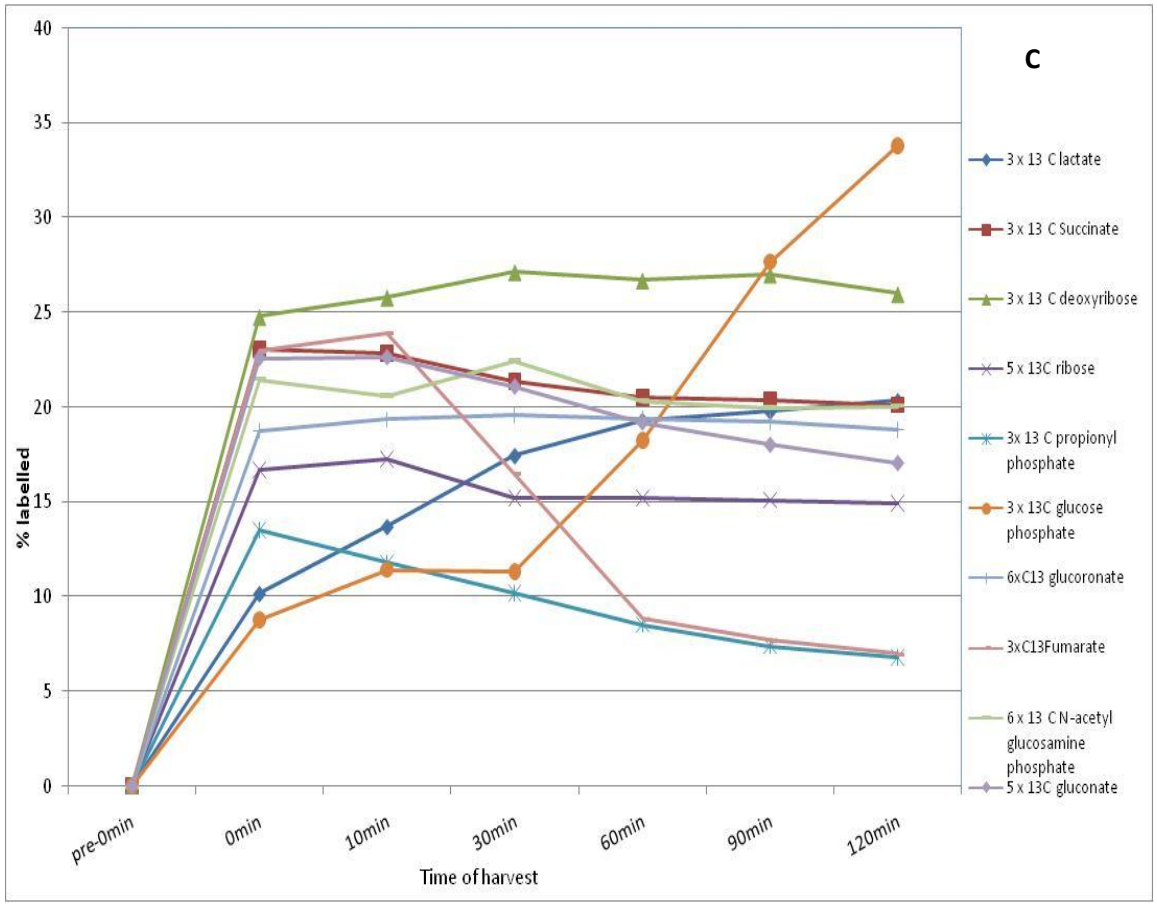

Figure 2.10: C shows levels of labelled metabolites obtained during incubation for 2hrs. In general, labelling started to level off after 60min. Pre-0min refers to diluted culture, i.e., before incubation at high density, where only unlabelled metabolites could be seen as shown in the previous graphs.

2.4.2 Discussion

In the experiment where $^{13}C_6$ glucose was added immediately prior to high density incubation the label incorporation into the metabolome was less extensive than where the cultures had been cultured with it from the outset. As can be seen in Figure 2.9, which represents sums of labelled and unlabelled for a single metabolite, all the metabolites started at low levels before the addition of $^{12}C_6$-glucose + $^{13}C_6$-glucose. Addition of glucose triggers off an increased rate of metabolism where levels of most metabolites increase rapidly to a plateau in the very short period between addition of glucose and sampling. The only metabolite shown in Figure 3.8 experiencing a lag was PEP which did not start to rise until 30 min. Glycerol phosphate levels decreased rapidly after 10 min implying its contribution into other pathways such as phospholipid biosynthesis or it being converted into glycerol and used in glycolysis. Pyruvate increased very rapidly in the first few minutes after addition of glucose but then decreased slowly up to 2 hours. For some metabolites, such as lactate and deoxyribose, incorporation of labelling took place very gradually before reaching a steady state. For others, incorporation of ^{13}C was very fast and as high as 50% or even 80% but then levelled off (Figure 2.10). This state of equilibrium in labelling after 60 min indicates that either the cells had stopped growing or that the label was being incorporated into other metabolites. Some metabolites which had been labelled in the experiment with long terms exposure to ^{13}C-glucose were detected but did not show any incorporation of labelling. Uridine, nonulose, AMP, octulose phosphate and glucosamine phosphate which had been labelled in the high density cultures were not labelled in this experiment. Propionate and propionate phosphate were not detected in these cultures even though they had been abundant in the previous experiment. This indicates that labelling of some compounds is much slower than others, the glycolytic metabolites are rapidly labelled but the purines which are required in DNA biosynthesis are much more slowly labelled over a short time period.

Further support for the transamination of pyruvate with glutamate to produce alanine can be observed in the data from the 2 h incubation experiment where the initial concentration of α- ketoglutarate in the FCS free growth medium is almost 0 and rises about 100 times during the 2h incubation and there was a concomitant reduction in glutamate levels (Figure 2.11) . The levels of alanine in the pellets, both labelled and unlabelled, rises markedly during the 2 h experiment.

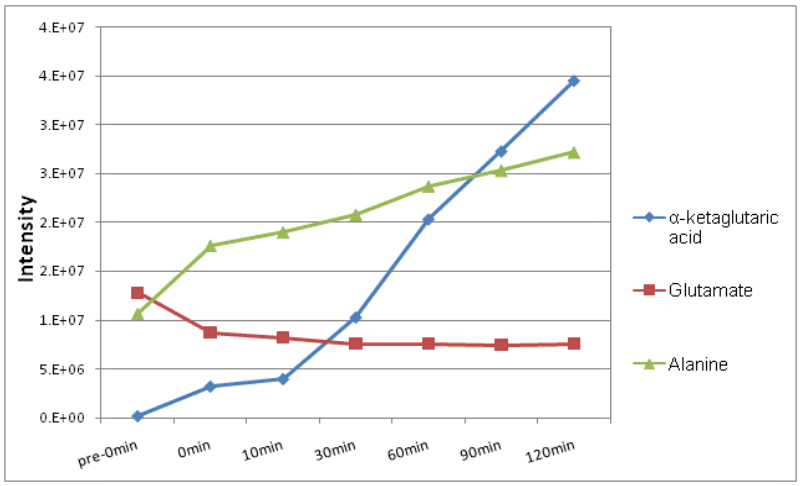

Figure 2.11.: The patterns indicate the transferring of amino group from glutamate to be converted to α-ketoglutarate.

Under incubation conditions, in Eppendorf tubes, trypanosomes would be metabolising towards anaerobic conditions which can be indicated to by increasing levels of glycerol, Figure 2.9 (B), which started from zero in diluted cultures up to 1.8E+6 at 2hrs (Eisenthal and Panes, 1985; Hammond and Bowman, 1980).

2.5 GC-MS Analysis in order to confirm the identity of key metabolites

Krebs intermediates were of most interest to identify by GC-MS in order to further confirm the identity of the labelled metabolites. In some cases, there were potential isomers which were not clearly separated on the ZICHILIC column. Therefore, the library hits, NIST (Thermo, Austin, USA), as well as comparison with the spectrum of reference materials helped in identifying these metabolites. Both

unlabelled $^{13}C_6$-labelled samples were derivatized in addition to reference materials. However, sugars could not be identified easily as they gave different hits even reference materials gave multiple peaks for a single reference. Therefore, this will require more work to be done on temperature programming and the derivatization protocol. After identifying the peak of a compound, its spectrum was compared to a reference material and the NIST library. As was the case with LC-MS, the isotopically labelled metabolites co-eluted with the corresponding unlabelled molecules. Therefore, the detection of labelling was easy. Table (2.3.) lists unique masses for some metabolites and their isotope peaks which show the decrease in $^{12}C/^{13}C$ ratio indicating incorporation of ^{13}C into these metabolites. Figures 2.12-2.15 show some examples of labelled metabolites.

Table 2.3: base peaks for some metabolites and the isotope ratio (lab/unlab) for their labelled peaks.

Name	**Unique mass**	**^{12}C-sample** ratio	**^{13}C-sample** ratio	**Name**	**Unique mass**	**^{12}C-sample** ratio	**^{13}C-sample** ratio
Lactate	117	1	1	Succinate	247	1	1
	119	20	2.85		250	50	2.6
	191	1	1	Glycerol	205	1	1
	193	10	2.8		207	10	1
	194	50	14.3		208	50	5.5
Alanine	116	1	1	Pyruvate	217	1	1
	118	20	1.2		218	5	4
	119	100	12.5		219	10	6.6
					220	50	1.25

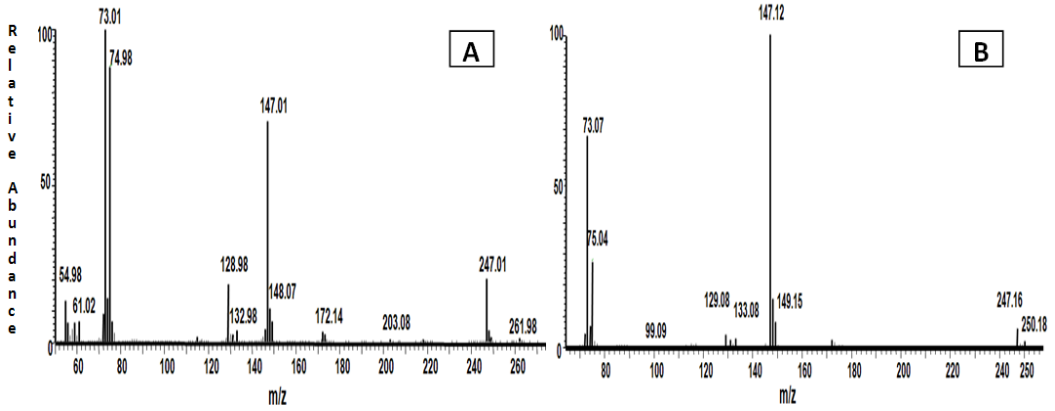

Figure 2.12.: A, succinate reference material showed a lower abundance for 250 m/z, whereas **B** shows the presence of 250 m/z indicating $^{13}C_3$-Succinate,

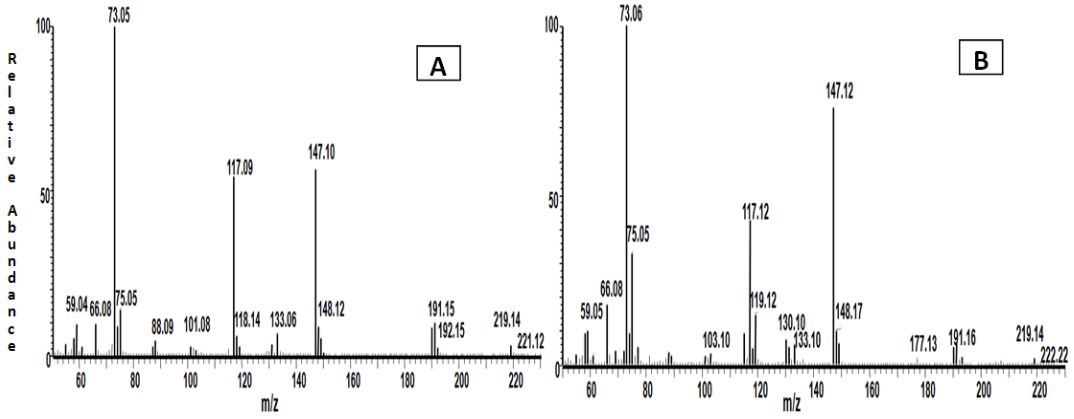

Figure 2.13.: A, lactate standard has a less abundant 119 ion whereas B has a higher abundance of 119 along with 117.

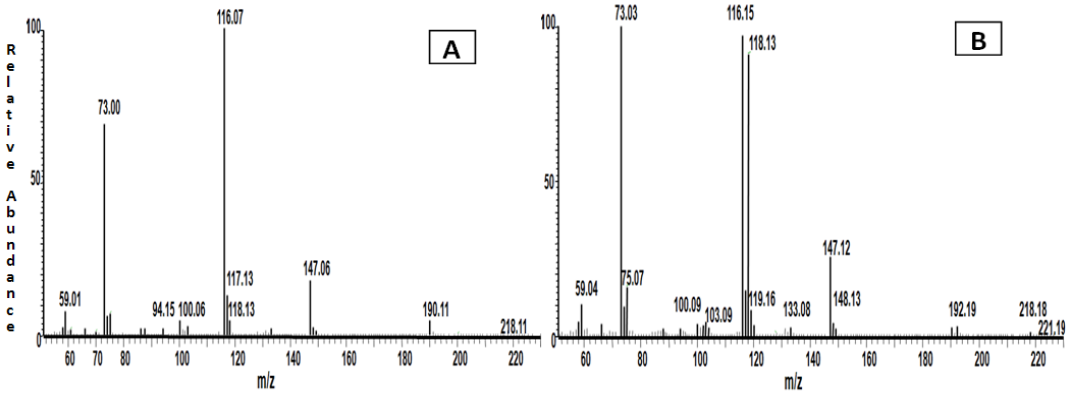

Figure 2.14.: Alanine in the ^{13}C-sample, B, shows 80% abundant mass at m/z 118, which to contributes to 5% of the base peak, 116, in the reference material spectrum, A.

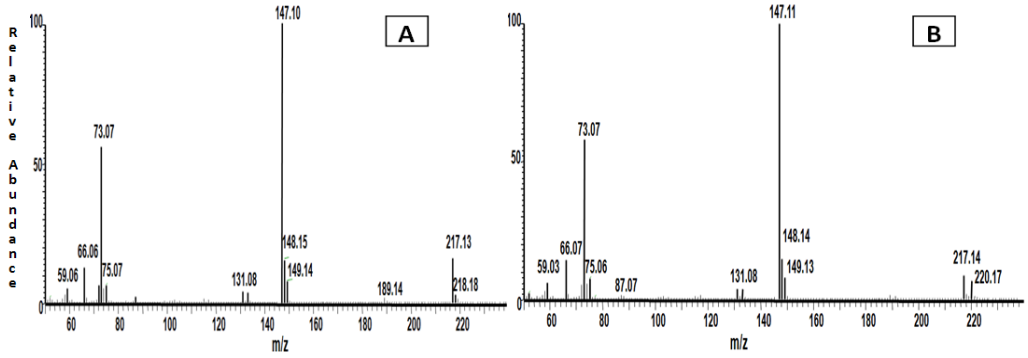

Figure 2.15.: Pyruvate in the ^{13}C-sample, B, shows 80% abundant mass at 220, however in the ^{12}C-samples,A , this peak was only 2%.

Since succinate was one of the important metabolites observed in order to differentiate between succinate and methyl malonate, an isomer of succinate, we ran reference materials for each on the GC-MS since these compounds were not separated by LC-MS on the ZICHILIC column. The fragmentation patterns did not readily differentiate them but they eluted at different retention times. Succinate eluted at 10.9 min whereas methylmalonate eluted at 8.8 min. The former matches the compound that was present in the samples. Similarly alanine was differentiated from β-alanine where they showed different retention times, alanine at 6.54min and β-alanine at 8.29min. These compounds do separate in the LC-MS system but in some samples analysed there was a retention time shift effect, probably due to traces of salt from the growth medium, where it was not possible to decide if the peak observed was due to alanine or β-alanine. Thus GC-MS with its high degree of chromatographic resolution provides a useful confirmation of identity where isomers are possible.

2.6 Minimal handling procedures following incubation for 24 and 48

Figure 2.16 (A, B and C) shows the plots for the labelling of the trypanosome metabolome at 24 and 48 hours after subculture. In an attempt to exclude factors that might have been involved in triggering BSF to switch to stumpy form metabolism a sample preparation protocol with minimal handling procedures was used by excluding the washing steps as well as the high-density incubation step. Therefore, after cultivation with $^{13}C_6$-glucose, the culture was spun for 10 min then the cells, with a little of the medium, were quenched into hot ethanol. The metabolome of BSF was analysed after 24hr and 48hr incubation with $^{13}C_6$-glucose starting from the point of subculturing into fresh medium. These cultures were diluted compared to high density cultures. In this set of experiments, propionate was not detected even after 48hrs. Octulose phosphate was neither detected at 24hrs nor after 48hrs nor NAD+. Incorporation of labelling into adenosine was only seen after 48hrs. Propionate was detected only in very low concentration as it accounted for only 1.3% of the levels of ^{13}C-pyruvate indicating that trypanosomes might produce it in response to a specific trigger such as anaerobic conditions. Succinate, malate, latate and fumarate were present as well. Succinate was the most abundant among them (about 52% of ^{13}C-pyruvate) whereas malate, lactate and fumarate were at 15%, 5% and 27%of the ^{13}C-pyruvate levels, respectively. On that account it would seem that BSF produce these metabolites and they were not products of their transformation into other forms but may be a response to the environmental conditions of the cultures. NAD+ was not detected which may be due to the fact that these cultures were about 5-times diluted compared to the high-density cultures. Similarly, sedoheptulose phosphate was not detected. Some metabolites did not show any labelling although they had been labelled in the high density culture e.g. uracil and alanine which again might be due to the diluted nature of the extracts. Labels were not incorporated into gluconic acid, nonulose phosphate and octulose phosphate.

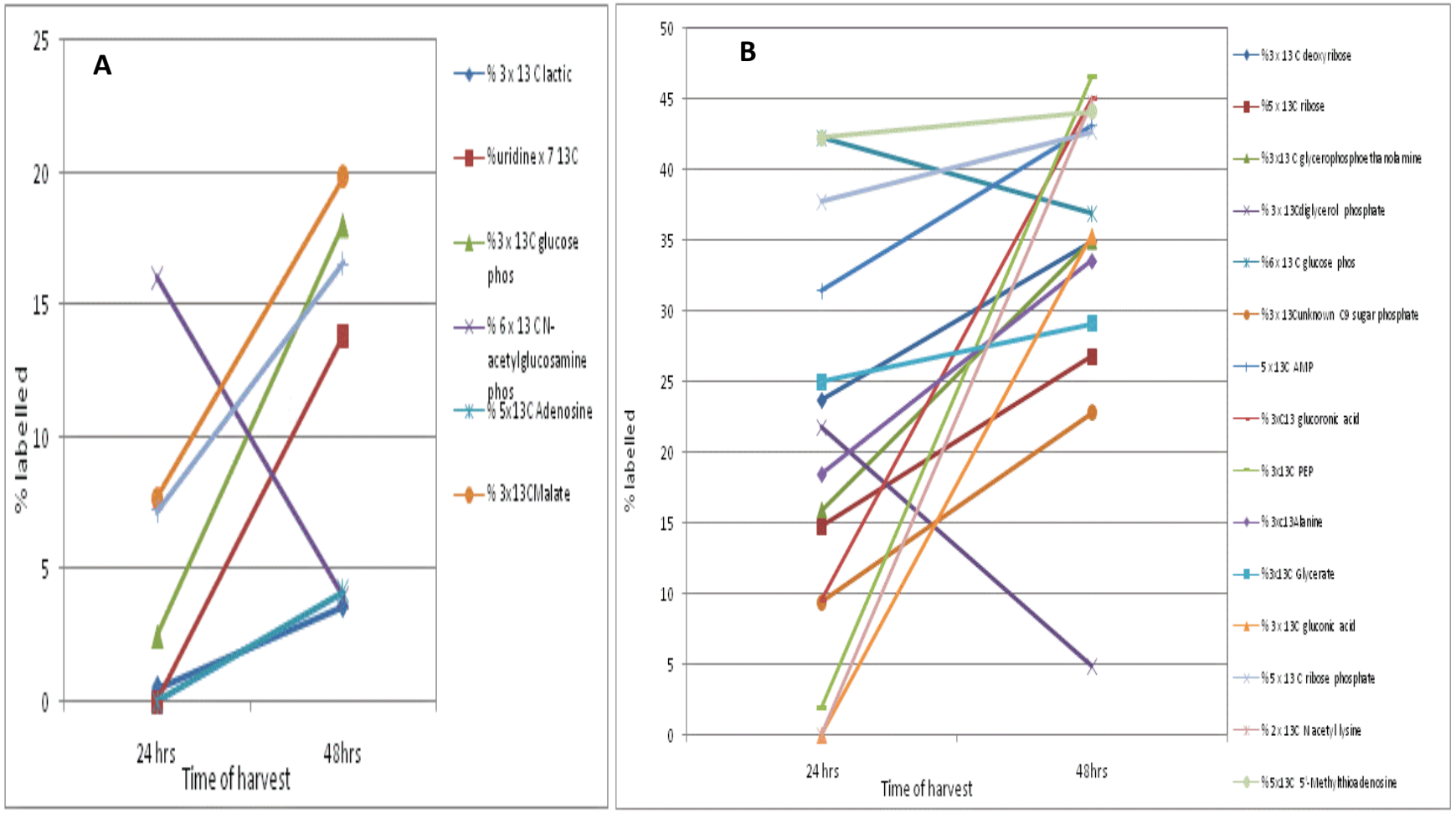

Figure 2.16: A and B levels of incorporation of labelling at 24 and 48hrs after incubation with $^{13}C_6$-glucose.

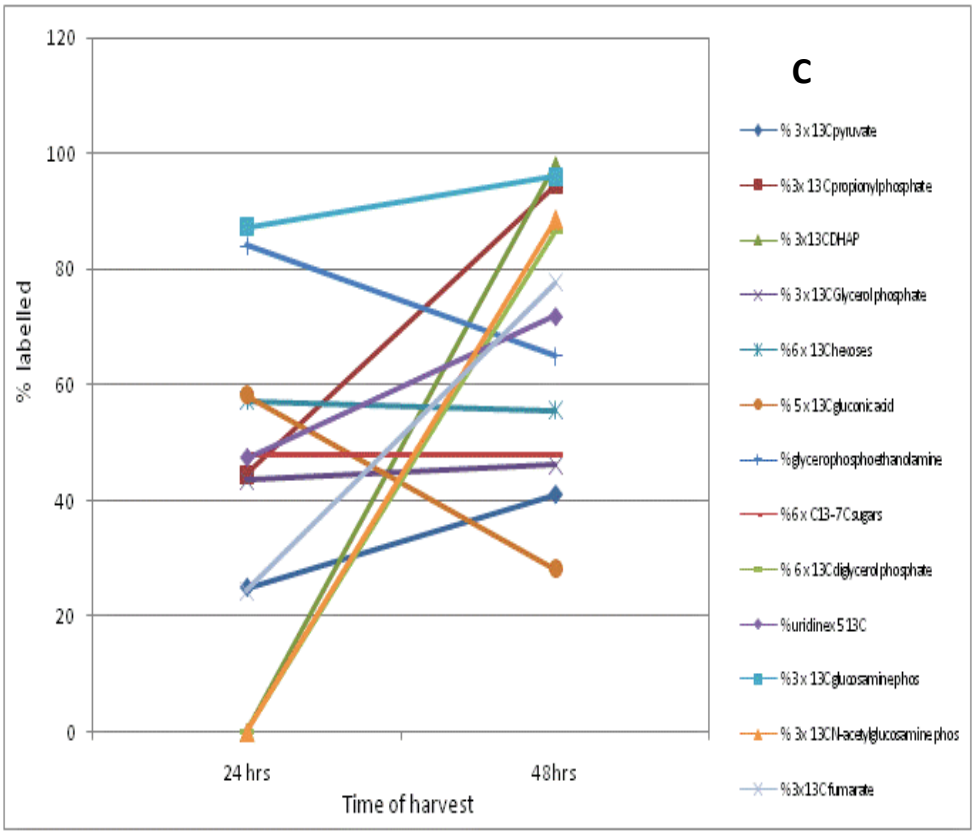

Figure 2.16.: C, incorporation of labelling in some metabolites after 24 and 48hr incubation with $^{13}C_6$-glucose.

After 24hrs, glyceric acid levels (which are thought to reflect dephosphorylated 3-phosphoglycerate which is an unstable compound) decreased significantly which indicated its incorporation into pyruvate which showed more than 3 fold increase in its levels at 48hrs compared to 24 hrs. On the other hand, DHAP and fumarate showed incorporation of label as high as 100% and 80% at 48hrs, respectively. Thus it would appear that the metabolism triggered by the high density incubations is unusual in comparison to the metabolism under normal culture conditions. However, the high density cultures do provide new data on the metabolic pathways available in trypanosomes. It would appear that some of the metabolic pathways observed under the high density incubations are activated as the density of the cultures increases.

2.7 Examination of alternative methods for quenching metabolism

Quenching cell pellets into acetonitrile (ACN) instead of hot ethanol was carried out to investigate whether hot ethanol might break down some metabolites leading to creation of other masses, especially in case of TCA metabolites. However, all Krebs cycle metabolites detected previously were seen excluding the effect of hot ethanol on breaking down some metabolites into masses matching these unexpected metabolites. On the other hand, phosphates in general, did not show good solubility in ACN as they were not detected. Furthermore, alanine was not detected. In general, detectable metabolites were shown to have lower levels compared to the samples extracted with hot ethanol reflecting their solubility preferences (data not shown).

CHAPTER [3]

LABELLING THE *T. BRUCEI* METABOLOME WITH DEUTERIUM

3. Deuterium labelling of the metabolome of *T.brucei*

3.1. Introduction:

In order to try and clarify the biosynthetic route producing the $^{13}C_3$-labelled Krebs cycle metabolites fumaric, succinic and malic acid observed in trypanosomes, cultures were incubated at high density in deuterated water. It was hoped that determining the number of protons incorporated into the metabolites might give some indication of the biosynthetic origin of these metabolites. From the results obtained with $^{13}C_6$-glucose labelling it was proposed that the Krebs cycle metabolites could either arise through the propionate pathway or via conversion of phosphoenol pyruvate into oxaloacetate, Appendix III.

Labelling by deuterium (^2H) has been used to provide information about kinetics and mechanisms of enzymatic reactions as well as the participation of the medium in which organisms are grown. In addition, some predicted biosynthetic pathways can be confirmed through incorporation of deuterium (Saur *et al.*, 1968). However, there are some reports of bacteria grown in D_2O containing medium showing growth retardation and morphological changes (Johnstone *et al.*, 1961; Marley *et al.*, 2001; Nevo *et al.*, 2004). In addition, genotypical changes might occur as a result of incorporation of deuterium into the DNA leading to errors during DNA replication (Bachner *et al.*, 1964). Moreover, growth in such medium may induce hyperosmoic stress into the cells (Nevo *et al.*, 2004). With this in mind it was decided that it would be better not to use 100% D_2O in the culture medium.

3.2. Cell culture and sample preparation

Cells were sub-cultured in HMI-9 medium which contained 1:4 D_2O/ H_2O for about 48hrs until they reached a density of $2.3x10^6$. Cultures were spun for 10min at 3000rpm at room temperature. Cell pellets were washed with 5mL of the H_2O medium then incubated with about 400µl of the D_2O medium for 30min at 37°C.

Cells were spun down and both cells and supernatant were quenched into hot ethanol at 80˚C, for 2min and then in ice for 3min. After spinning them for 3min at 13000rpm at room temperature, supernatant was stored at -80°C until analysis time. Control cultures were treated in the same way using medium containing H_2O .

3.3. Results

Figure 3.1: Expected incoroporation of label into succinate and propionate

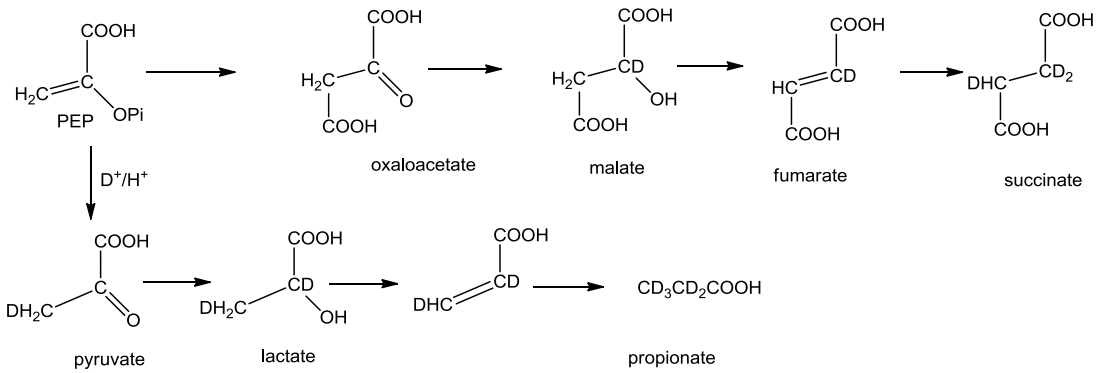

On the day of harvesting, the cell count of cultures grown in D_2O medium was less than that of those grown in H_2O suggesting that D_2O might have some growth inhibition effect on the cells as mentioned earlier. Figure 3.1 shows the pathways of interest in trypanosomes for incorporation of deuterium into succinate and propionate. Chromatograms of labelled samples showed higher relative abundances of $^{2}H_1$-labelled peaks compared to H_2O samples, Figures 3.2 and 3.3 Single labelled peaks were found to be much higher than double labelled where most of the metabolites of interest did not show much double labelling. Most of the labelled peaks are either absent or very low in the H_2O medium. Table 3.1 shows the detected peaks with their ^{2}H-labelled counterparts along with their %relative abundance compared to parent compounds which accounted for 100%. The data obtained are difficult to explain and from this preliminary experiment it is difficult to be definitive about what is occurring. Nonetheless the labelling patterns do raise some interesting questions about the exact biosynthetic route for these compounds. Pyruvate was abundant as expected and carried a single deuterium label, the monodeuterated peak is clearly separated from the $^{13}C_1$-of pyruvate and

the incorporation of deuterium into pyruvate was 22% (Table 3.1). The label incorporates into the methyl group of pyruvate when a deuterium/proton attacks the double bond in phosphoenol pyruvate along with the transfer of one mole of phosphate to ATP. The level of label incorporation in this case is in line with that which would be expected from the % of D_2O in the growth medium. In contrast the level of label in lactate is low with only 4% becoming monodeuterated, it would be expected that the reduction step between pyruvate and lactate would introduce an extra deuterium. It would seem that lactate does not come from pyruvate in this case. However, propionate is monodeuterated to a similar extent as pyruvate and would normally come via lactate (Appendix III), it could in theory be up to trideuterated (Figure 3.1) . Succinate is monodeuterated to a similar extent as pyruvate but it might be expected to have gained up to three deuteriums. The anomalies in labelled patterns can be explained by the kinetic isotope effect. To break a bond, a minimum vibrational energy (E_o) which is described in the equation below, is required:

E_o=1/2hv…… (Clayden *et al.*, 2001)

In this case the vibrational energy of C-D bond is lower than that of a C-H bond. Therefore, more energy is required to break a C-D bond which in turn makes the reaction rate of C-D slower than that of a C-H bond. Thus reduction reactions involving NADH or NADPH where deuterium is present rather than hydrogen are likely to be much slower since the proton present on the reduced pyridinium ring will transfer much more quickly. Pyruvate is labelled in line with expectation and in this case the label comes from a deuterium ion, which also has to be formed by the breaking of an O-D bond, labelling of many of the other compounds depends on NADD and the low degree of labelling definitely reflects the slow reaction of the C-D bond compared with the C-H bond.

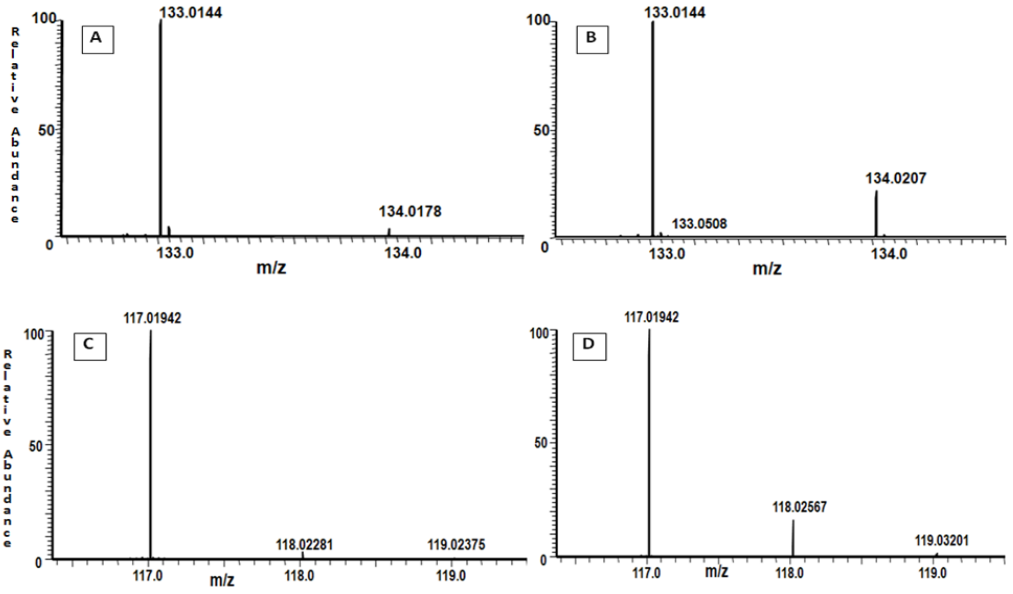

Figure 3.2 Chromatograms of malate and succinate in H_2O medium, A,C with their labelled peaks in D_2O medium, B and D.

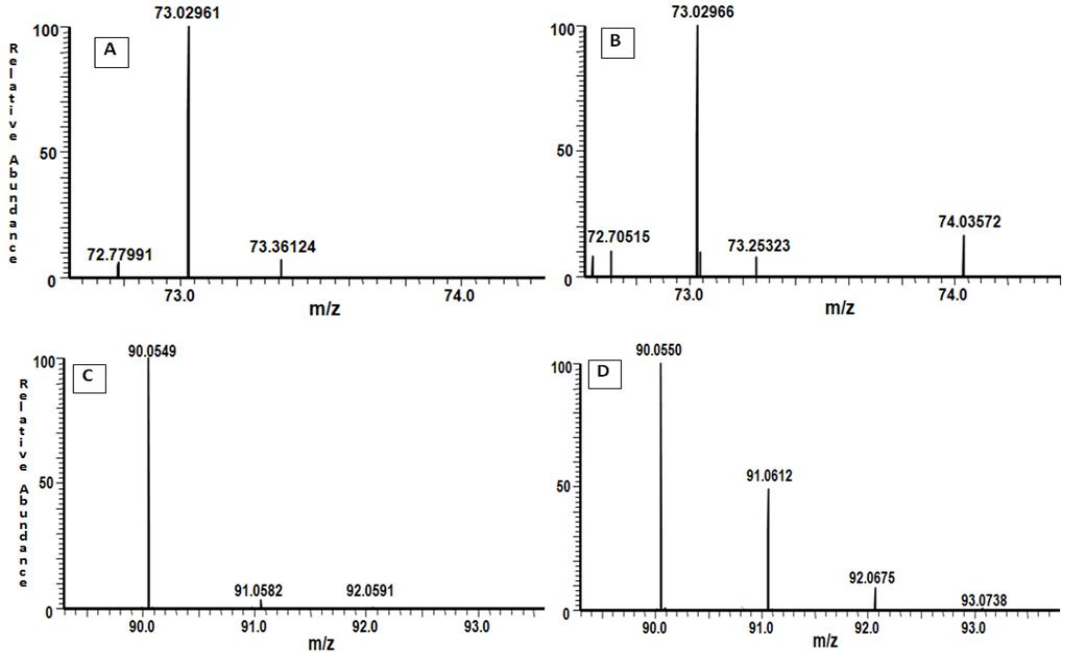

Figure 3.3: A and C represent unlabelled propionate and alanine whereas in B and D, incorporation of ^2H can easily be detected.

Table 3.1: a list of ^{2}H-labelled metabolites with their relative abundances.

Name	MZ	Time (min)	%Relative Abundance	Name	MZ	Time (min)	%Relative Abundance
Propionic acid	73.02958	6.7	100	gluconic acid	195.051	13.5	100
1x2HPropionic acid	74.03587	6.7	16	1x2H gluconic acid	196.0575	13.5	0.1
pyruvate	87.00871	7.6	100	glycerophosphoethanolamine	214.0491	14.7	100
1x2H pyruvate	88.015	7.6	22	1x2H glycerophosphoethanolamine	215.0555	14.7	0.32
lactic	89.02449	6.5	100	7 C sugars	225.0615	12.9	100
1x2H lactic	90.03078	6.5	4	1x2H 7C sugars	226.0651	12.9	similar to unlab
Succinate	117.0194	6.7	100	diglycerol phos	245.0434	14.3	100
1x2H Succinate	118.0256	6.6	20	1x2H diglycerol phos	246.05	14.3	0.58
2x2H Succinate	119.032	6.7	2	uridine	243.0627	10.2	100
glyceric acid	105.0194	7.6	100	1x2H uridine	244.0687	10.2	0.3
1x2H glyceric acid	106.0257	7.6	25	glucose phosphate	259.0224	16	100
2x2H glyceric acid	107.032	7.5	very little	1x2H glucose phosphate	260.0292	16	0.26
malic acid	133.0143	7.6	100	N-acetylglucosamine phos	300.0494	14.5	100
1x2H malic acid	134.0206	7.6	20	1x2H N-acetylglucosamine phos	301.0558	14.5	0.32

2x2H malic acid	136.0333	7.6	very little	unknown C8 sugar phosphate	319.044	17.45	100
deoxyribose	133.0508	7.0	100	1x2H unknown C8 sugar phosphate	320.0498	17.5	0.4
1x2H deoxyribose	134.0571	7.0	50	AMP	346.0564	15.3	100
ribose	149.0457	9.9	100	1x2H AMP	347.0627	15.4	0.32
1x2H ribose	150.0521	9.8	25	Glucoronic acid	193.0355	7.6	100
propionyl phosphate	152.9959	14.6	100	1x2H Glucoronic acid	194.042	7.6	0.56
1x2H propionyl phosphate	154.0022	14.6	35	2x2H Glucoronic acid	195.0486	7.6	0.1
glycerol phosphate	171.0066	15.4	100	fumarate	115.0037	8.2	100
1x2H glycerol phosphate	172.0129	15.4	28	1x2H fumarate	116.0099	8.2	0.1
2x2H glycerol phosphate	173.0192	15.7	2	Ascorbate	175.025	7.6	100
hexose	179.0563	12.9	100	1x2H Ascorbate	176.0313	7.6	0.54
1x2H hexose	180.0626	12.9	1	2x2H Ascorbate	177.0377	7.6	0.1

3.4. Discussion:

In conclusion perhaps mixing metabolomics, which is aleady complex, with quantum mechanics was not the best way forward. Thus in future other labelling strategies will be tried in order to find out which route trypanosomes use to produce $^{13}C_3$-labelled Krebs cycle metabolites. The conversion of PEP to pyruvate as expected incorporated one deuterium but lactate was hardly labelled at all and pyruvate, which was expected to arise via lactate, had about 16% labelling. Oxaloacetate was not observed and malate was labelled with one deuterium atom as would be expected if it comes directly from PEP via oxaloacetate. Formation of fumarate would be expected to retain the deuterium following dehydration but fumarate was not labelled. Succinate was mainly monodeuterated and it should have had up to three deuteriums incorporated (Figure 3.1). Thus the deuterium labelling experiment did not clarify matters but made them more confusing. It would seem on the current evidence that succinate does not arise from PEP via oxaloacetate.

3.5 Conclusion:

The labelling studies have raised more questions than they answer. However, it can be seen that labelling provided a simple method for probing the metabolism of trypanosomes and have indicated some unusual metabolic pathways which might be potential drug targets. The most interesting features are the formation of $^{13}C_3$-labelled succinate, the apparent importance of propionate as a metabolite and the formation of unusual metabolites in the pentose phosphate pathway via the action of ketoaldolase. Thus the current set of results is only a preliminary examination of trypanosome metabolism using this methodology. It will be quite difficult to establish the route of metabolism to succinate from glucose since labelling patterns via the two proposed routes, from PEP via oxaloacetate or via the propionate pathway, will produce similar labelling patterns. The next step will be to utilise ^{13}C-labelled propionate to probe the pathway.

CHAPTER [4]

PROPOLIS EFFECT ON *T. BRUCEI*

4.Incubation of *T. Brucei* with propolis

4.1Introduction:

Propolis is naturally produced by honeybees which use it to seal their hives and protect them from invaders. In addition, honeybees use this thick substance to cover dead invaders and this is thought to have something to do with eliminating any microbial contamination (Sawaya *et al.*, 2007). Therefore, the interest in using it as a therapeutic agent has increased significantly since it has been used as a natural remedy for different diseases for a long time (Burdock, 1998; Bankova *et al.*, 1995).

It is expected that the composition of propolis will vary according to the different sources that bees use to synthesise it. Commonly raw propolis is composed of 5% various organic acids, 5% pollen, 10% essential oils, 30% wax and about 50% resin. The latter often consists of flavonoids and phenolic acids which is collectively known as the polyphenolic fraction (Volpi and Bergonzini, 2006). Upon extraction, commonly with ethanol, mainly the polyphenolic fraction is obtained which is believed to be responsible for the antioxidant, antibacterial and antiviral effects of propolis (Havsteen, 2002). In addition, propolis has been found to have further biological activities including anti-inflammatory, anti-tumour, hepato-protective and anti-protozoan (Seidel *et al.*, 2008). There have been different studies indicating that propolis has a trypanocidal effect. Dantas and others studied the effect of propolis *in vitro* on skeletal muscle cells-infected with *Trypanosoma cruzi* where it was found to be active in terms of reducing intracellular proliferation of trypanosomes at a concentration 12.5 times less than that needed to damage host cells (Dantas *et al.*, 2006). In another study by Higashi and Castro, it was found that both ethanolic and DMSO extracts of propolis were effective against *T. cruzi*. Lysis of bloodstream form (BSF) trypomastigotes was observed after 24hr using an ethanolic extract at a concentration of 100μg/mL (Higashi and Castro, 1994). This study showed that the trypanosomes were suffering from oxidative stress which was reflected in the increased levels of trypanothione disulfide (the oxidized form of trypanothione ($T(SH)_2$)) as a result of adding propolis. Trypanothione is a unique

thiol which is detected in some trypanosomatidae species, its function is protection of trypanosomes against oxidative stress through oxidation into the disulfide form which is followed by regeneration of trypanothione by trypanothione reductase, Figure 4.1, hence, the redox balance is maintained (Jones *et al.*, 2010). Trypanothione reductase is found only in trypanosomes but not in human cells which makes it a preferred target for drug discovery (Spinks *et al.*, 2009).

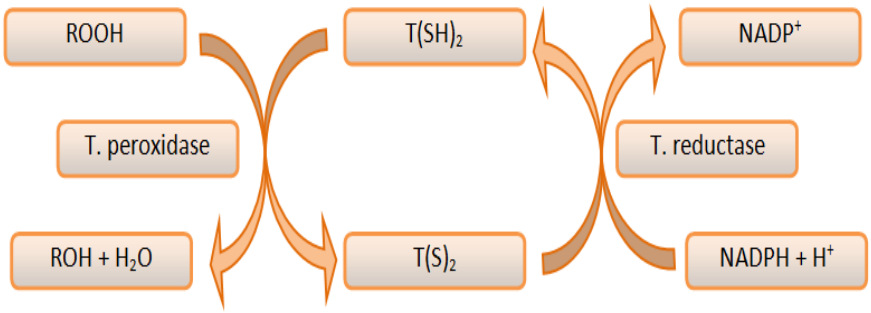

Figure 4.1.: Trypanothione reductase activity.

In the current study, an extract from propolis collected in Africa was added to BSF trypanosomes cultured in HMI-9 medium enriched with 10% FCS. The IC_{50} was determined using the Alamar Blue (AB) test. Finally, a metabolomic study was carried out to investigate the effect of the propolis on the metabolome using the 50% inhibitory concentration IC_{50} and a higher concentration to see its effect on trypanosomes in a fully grown culture. The particular propolis tested had been found to be very potent (Seidel *et al.*, 2008) and it was of interest to try and gain an understanding of whether a metabolic system within the trypanosomes was selectively affected by it targeting a particular pathway.

4.2Materials and methods

4.2.1 Propolis extract:

A crude sample of propolis was collected in Africa in 2006 and stored in a cool dark cupboard. The sample was cut into small pieces and 50 g were extracted with a

mixture of acetone and methanol at room temperature resulting in 80% w/w yield. Then the extract was filtered, evaporated to dryness under vacuum and the residue was dissolved in DMSO and then stored at -20°C.

4.2.2 Alamar Blue Test:

The test was carried out in a 96-well micro titre plate. 100µL of HMI-9 medium containing 10% FCS were added to each well and a serial dilution of the propolis extract ranging from 100µg/mL to 2.38E-05µg/mL was used. A negative control was used in addition to a positive control of pentamidine (Sigma, UK) in a concentration range of 200 µM to 4.77E-05µM. DMSO was also added as a control to exclude its effect. Then 100µL of BSF trypanosomes (427WT) at a concentration of $4x10^4$cells/mL was added to each well. Plates then were incubated for 48hrs at 37°C. Then 20µL of Alamar Blue (0.49 mM in 1X PBS, pH 7.4) was added to each well then the plates were incubated again for 24hrs. Readings were taken using a FLUOstar OPTIMA (LABTECH, Offenburg, Germany). The IC_{50} value was calculated using Prism software, version 5 (GraphPad, USA). The plates were checked every 1hr for the first 6hrs then at 24Hr and at 48hrs.

4.2.3 Metabolomics experiment:

Cultures of BSF trypanosomes (427WT) were used at a concentration of 1.95×10^6 cell/mL. Propolis was added to cultures at concentration equal to the IC_{50} and in a higher concentration of 50µg/mL and then incubated. Harvesting was carried out 1hr and 2hr after adding propolis. Control cultures were set up by adding DMSO in quantities equal to that used for inoculating propolis into cultures. Analysis of samples by LC-MS was performed according to the protocol described in section 2.2.

4.3 Results:

4.3.1 IC_{50} calculation

After performing the experiment three times the average readings were plotted on the graph (Figure 4.2). The IC_{50} was found to be within the range 3.4-3.8µg/mL . DMSO was shown to have no effect on the proliferation of the cells.

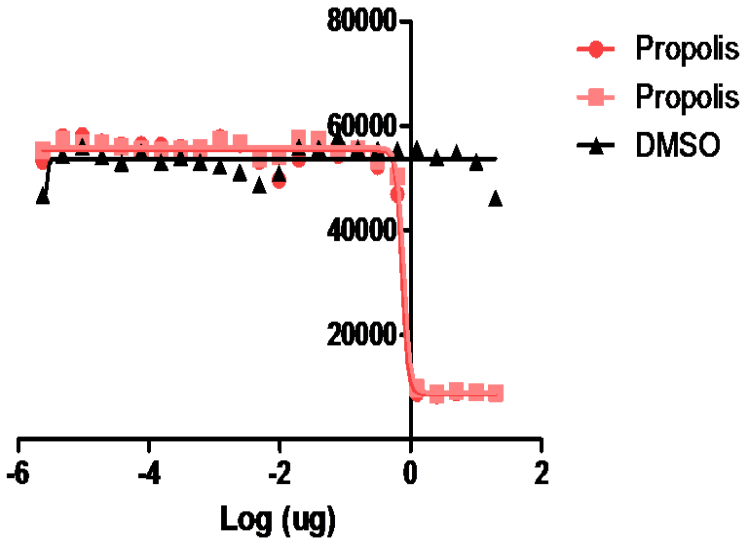

Figure 4.2.: Determination of propolis IC_{50} value compared to DMSO which had no effect on cell growth.

4.3.2 Time of death of cells

Following the setting of Alamar Blue experiment with propolis in concentrations from 100-2.38E-05 µg/mL , the first set of plates indicated early cell death which suggested that the cells were stressed and a change in temperature affected them significantly. This led to death of cells after 24hr in a random pattern with regard to propolis concentration. Therefore, it was decided to check only wells where the propolis concentration was around the IC_{50} value. After 1hr incubation, the cells exhibited normal motility. However, after 2hrs, cells in the first four wells died

(concentration range from 12.5 to 100µg/mL). The fifth well, on the other hand, had few dead cells with many surviving cells. This pattern continued for the next 2hrs with the complete death of the cells in the fifth well at 6hr incubation and at 24hrs.

4.3.3 Metabolomics experiment at IC_{50} and 50µg/ml propolis extract

In this experiment, cells were incubated with two different concentrations of propolis including IC_{50} and a higher concentration of 50µg/mL. When cells were incubated at the IC_{50} value after one hour incubation, the cells were shown not to be affected, however, after 2hrs incubation, the motility of the cells was slower than that of DMSO cultures. Upon adding propolis at 50µg/mL and incubating the cultures for 1hr, a significant cell death was observed, although cultures incubated with DMSO showed no effect. After two hours, cells in cultures incubated with propolis were almost all dead, i.e., not moving, in contrast to cultures incubated with DMSO which continued to grow normally.

4.3.4 Metabolite changes

4.3.4.1 Purines and Pyrimidines

Many metabolites underwent a reduction in their levels upon the addition of propolis with marked reduction in the levels of putrescine, AMP, guanosine and xanthine. The only metabolite which increased was xanthosine. It is difficult to say if these changes mark selective effects on a particular pathway or are just indicative of cell death, table 4.1.

4.3.4.2 Lipids

Metabolites involved in choline biosynthesis were decreased in levels following treatment with propolis although choline itself was not significantly affected. Lysophosphocholine lipids were increased significantly after treatment with propolis most of which are thought to be involved in cell membrane structures, see

Table 4.1: Ratio of some metabolites in propolis treated cultures compared to DMSO cultures. These values represent metabolic changes using a 50µg/mL concentration of the propolis. First column shows the ratio of levels of metabolites after 2hr incubation with propolis.

Compounds	1hr(prop/DMSO)	2hr(prop/DMSO)
Putrescine	0.13	0.01
Cytosine	1.38	0.81
Thymine	0.60	0.58
L-Ornithine	0.53	0.54
Adenine	0.32	0.33
Hypoxanthine	0.66	0.73
Xanthine	0.13	0.24
(S)(+)-Allantoin	0.91	0.78
Thymidine	0.56	0.53
Adenosine	0.65	0.86
Guanosine	0.06	0.14
Xanthosine	0.92	2.18
Methyldihydroinosine	0.53	0.65
AMP	0.02	0.07

Table 4.2. These may be indicative of membrane breakdown and the depletion of glycerol and choline phosphate may indicate that the cells are trying to repair the damage produced by the treatment with propolis.

Table 4.2: A list of lipids detected in positive mode of analysis and their ratios in propolis/DMSO treated samples. These changes were observed at a propolis concentration of 50µg/mL.

Compounds	1hr(prop/DMSO)	2hr(prop/DMSO)
Choline+	0.61	0.73
Diethanolamine	1.14	1.16
Glycerolphosphate	0.09	0.06
Choline phosphate+	0.06	0.02
phosphoethanolamineR	0.23	0.77
glycerylphosphocholine	0.19	0.09
Dehydrosphinganine(Sphingosine)	50.83	47.08
Myristoyl L-α-lysophosphatidylcholine	39.40	9999
1-(9E-hexadecenoyl)-sn-glycero-3-phosphocholine	9.98	6.00
1-Palmitoyllysophosphatidylcholine	4.80	3.52
1-(9Z-heptadecenoyl)-sn-glycero-3-phosphocholine	162.43	9999
1-heptadecanoyl-sn-glycero-3-phosphocholine	15.40	8.14
1-Linoleoylglycerophosphocholine ,1-Linoleoylphosphatidylcholine	9.23	4.60
1-Oleoylglycerophosphocholine ,Oleoyl lysophosphatidylcholine	8.01	5.81
1-Stearoylglycerophosphocholine ,1-Stearoyl-sn-glycero-3-phosphocholine	4.58	3.50
N-Palmitoylsphingosine ,Ceramide (d18:1/16:0)	2.07	2.95
1-(8Z,11Z,14Z-eicosatrienoyl)-sn-glycero-3-phosphocholine	34.16	58.18

4.4 Other changes

Some amino acids as shown in Table 4.3, had reduced levels after addition of propolis although their levels had not changed over a two hour incubation. Moreover, citrulline levels increased by more than 10 times of that of DMSO cultures although intensity of the peak is low compared to other aminoacids and this corresponds with the lowered level of arginine in the treated cultures and the decrease in putrescine. Conversion of arginine into citrulline is an alternative to its conversion into ornithine and from ornithine into putrescine. The presence of low levels of porphyrins in the treated cultures is almost certainly a mis-identification since these

compounds are quite high MW and thus the number of possibilities for sensible elemental compositions is high.

Table 4.3: Other metabolites and their ratios in propolis samples compared to DMSO.

Compounds	1hr(prop/DMSO)	2hr(prop/DMSO)
Alanine	0.39	0.47
L-Proline	0.60	0.65
L-Ornithine	0.53	0.54
Carnitine	0.35	0.47
L-Citrulline	12.65	12.46
L-Arginine	0.67	0.72
protoporphyrin IX	567.40	9999
Mesoporphyrin IX	9999	730.69
Protoporphyrinogen IX	9999	509.10

4.4 Incubation of trypanosomes with propolis at the IC_{50} concentration

When fully grown cultures were treated with propolis at the IC_{50} level there were fewer significant metabolic changes except that there was a 50% reduction in levels of purines compared to negative control cultures as shown in Table 4.4. This in total suggests that the incubation was not enough to study these changes as the experiment was done over two hours only. Further work is thus required to determine whether or not the propolis extract is selectively targeting a particular area of the parasite's metabolism but the preliminary work has shown that this might be a useful addition to the development of this treatment. If the toxicity of the propolis is selective then it might be a viable treatment since there needs to be a reasonably large therapeutic window between toxicity to the parasite and toxicity to its hosts.

Table 4.4: List of purines and pyrimidines and their levels upon addition of propolis at IC_{50} concentrations compared to negative control cultures.

Compounds	prop_1h/Ctrl	DMSO_1hr/Ctrl	prop_2hr/Ctrl	DMSO_2hr/Ctrl
(S)(+)-Allantoin	1.10	1.12	0.91	1.02
Adenine	1.20	1.53	2.21	1.47
Adenosine	0.31	0.77	1.46	0.61
Allantoate	0.69	0.56	0.71	0.54
AMP	1.28	1.56	2.67	1.77
Guanosine	0.61	0.63	0.53	0.66
Hypoxanthine	0.63	0.61	0.61	0.65
Inosine	0.57	0.67	0.57	0.48
L-Glutamine	0.69	0.65	0.70	0.69
Nicotinamide	0.56	0.55	0.52	0.57
Thymidine	0.56	0.48	0.51	0.47
Thymine	0.56	0.51	0.54	0.49
Uracil	1.14	1.56	1.66	2.30
Uridine	0.70	0.66	0.84	0.77
Xanthine	0.61	0.67	0.61	0.87

4.5 Discussion

LC-MS analysis revealed many changes in the cell metabolome of the cultures incubated with propolis starting with a significant reduction in levels of most metabolites which refers to either impairment of certain enzymes within surviving cells or death of the majority of cells in a short time. Such effects may be due to a generalised toxicity and thus not particularly useful since the sample would be likely to be cytotoxic at such concentrations. However, there was a significant depletion

of trypanothione disulfide ($T(S)_2$), a selective trypanosome metabolite, compared to samples treated with DMSO only, Figure 4.3 Under the extraction conditions used $T(SH)_2$ is converted to $T(S)_2$ and $T(S)_2$ is taken as representing total trypanothione. Thus the fall in the levels indicates that the treatment is in some way interfering with the production of total trypanothione by the cells. This might be via a specific interference with trypanothione biosynthesis of just through a generalised toxicity against the cells. In addition, there were high levels of lipids in the propolis-treated cultures which might reflect one of the cells' defensive mechanisms against toxicants or attempts to repair damage that happens under oxidative stress (Uzcategui *et al.*, 2007). When propolis at the LD_{50} level was used in the treatment a more subtle toxicity effect was produced where mainly purines were affected by the treatment, this effect requires further investigation. The sample of propolis used was the unrefined version and further purification of the sample has increased in potency so that it is effective in the sub-microgram range. The metabolomics testing will continue by examining this purified material.

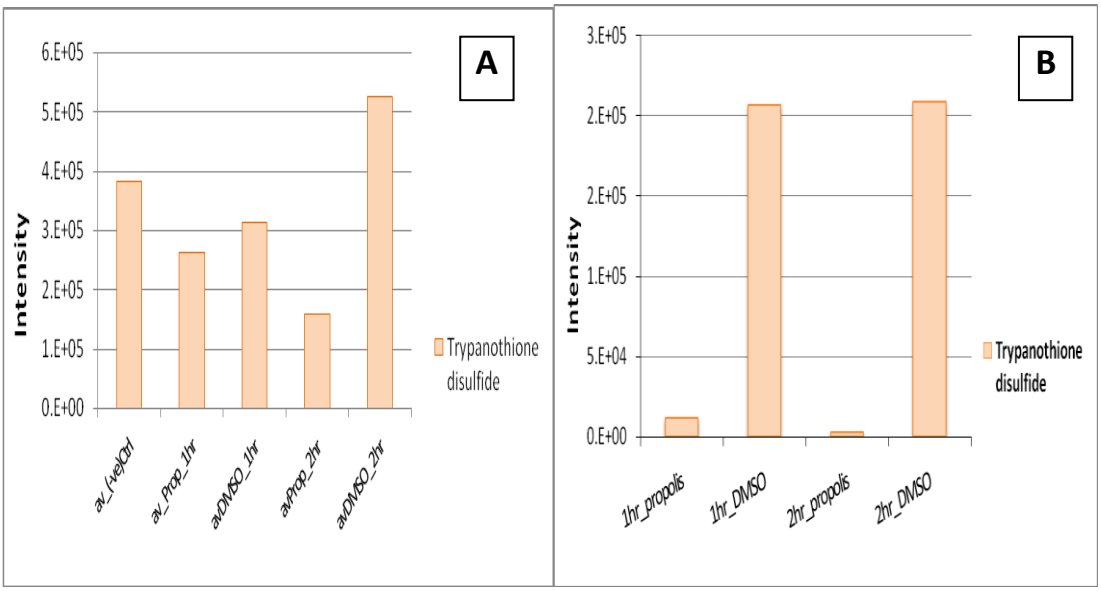

Figure 4.3: A: decreasing levels of $T(S)_2$ using IC_{50}. B: significant depletion of $T(S)_2$ using 50µg/mL propolis compared to DMSO cultures.

4.6 Conclusion

Using propolis as a trypanocidal agent may be a promising approach. However, its exact effect needs to be extensively studied in order to understand its mechanism of action on the biochemical level. This can be carried out by using LC-MS and GC-MS where many metabolites can be easily detected and significant changes can be instantly observed. Therefore, it would be more meaningful to study incubation of trypanosomes with propolis for longer time and applying different concentrations. Furthermore, if the active constituents are separated from the crude extract and used directly, more specific results might be obtained which might indicate a specific toxicity mechanism.

5. References

Albert, M. A., Haanstra, J. R., Hannaert, V., Van Roy, J., Opperdoes, F. R., Bakker, B. M. & Michels, P. A. (2005). Experimental and in silico analyses of glycolytic flux control in bloodstream form *Trypanosoma brucei. Journal of Biological chemistry* **280**: 28306-28315.

Albert, M. A., Haanstra, J. R., Hannaert, V., Van Roy, J., Opperdoes, F. R., Bakker, B. M. & Michels, P. A. (2005). Experimental and in silico analyses of glycolytic flux control in bloodstream form *Trypanosoma brucei. The Journal of Biological Chemistry* **280**: 28306-28315.

Bachner, P., McKay, D. G. & Rittenberg, D. (1964). The Pathologic Anatomy of Deuterium Intoxication. *Proceedings of the National Academy of Sciences of the United States of America* **51**: 464-471.

Bajad, S. & Shulaev, V., (2007). Highly-parallel metabolomics approaches using LC-MS for pharmaceutical and environmental analysis. Trends in Analytical Chemistry **26**: 625-*636.*

Bajad, SU, Lu W, Kimball, EH., Yuan, J., Peterson, C. & Rabinowitz, JD. (2006). Separation and quantitation of water soluble cellular metabolites by hydrophilic interaction chromatography-tandem mass spectrometry. *Journal of Chromatography A* **1125**:76–88.

Bankova, V., Christov, R., Kujumgiev, A., Marcucci, M. C. & Popov, S. (1995). Chemical composition and antibacterial activity of Brazilian propolis. Zeitschrift für Naturforschung C **50**: 167-172.

Bedair, M. & Sumner, L. W. (2008). Current and emerging mass-spectrometry technologies for metabolomics. *Trends in Analytical Chemistry* **27**(3): 238-250.

Beecher, C. W. W. (2003). The human metabolome. In:, *Metabolic profiling: Its role in biomarker discovery and gene function analysis*. Eds: Harrigan G. G. And Goodacre R. RG, *1st ed*, pp 311-320, USA, Springer.

Bringaud, F., Riviere, L. & Coustou, V. (2006). Energy metabolism of trypanosomatids: adaptation to available carbon sources. *Molecular and Biochemical Parisiteology* **149**: 1-9.

Burdock, G. A. (1998). Review of the biological properties and toxicity of bee propolis (propolis). *Food and Chemical Toxicology* **36**: 347-363.

Chen, C., Gonzalez, F. J. & Idle, J. R. (2007). LC-MS-based metabolomics in drug metabolism. *Drug Metabolism Reviews* **39**: 581-597.

Clayden, J., Greeves, N., Warren, S. & Wothers, P. (2001). *Organic Chemistry*. Oxford University Press, NY, USA, pp: 486-487.

Coustou, V., Biran, M., Breton, M., Guegan, F., Riviere, L., Plazolles, N., Nolan, D., Barrett, M. P., Franconi, J. M. & Bringaud, F. (2008). Glucose-induced remodeling of intermediary and energy metabolism in procyclic *Trypanosoma brucei. Journal of Biological Chemistry* **283**: 16342-16354.

Cubbon, S., Antonio, C., Wilson, J. & Thomas-Oates, J. (2009). Metabolomic applications of HILIC-LC-MS. *Mass Spectrometry Reviews* **29**: 671-684.

Cunnick, W.R., Cromie, J.B., Cortell, R., Wright, B., Beach, E., Seltzer, F. & Miller, S., (1972). Value of biochemical profiling in a periodic health examination program: analyses of 1,000 cases. *Buletin of New York Academy of Medicine* **18**: 5-22.

Dantas, A. P., Salomao K., Barbosa, H. S. & De Castro, S. L. (2006). The effect of Bulgarian propolis against *Trypanosoma cruzi* and during its interaction with host cells. *Memorias do Instituto Oswaldo Cruz* **101**: 207-211.

Dass C. (2001). *Principles and Practice of Biological Mass Spectrometry*. John Wiely and Sons, USA, pp: 64-65.

Davis, D. J., Burlak, C. And Money, N. P. (2000). Osmotic pressure of fungal compatible osmolytes. *Mycological Research* **104**(7): 800-804.

Dettmer, K. & Hammock, BD. (2004). Metabolomics—A new exciting field within the ‘‘omics’’ sciences. *Environmental Health Perspectives* **112**:A396–397.

Dettmer, K., Aronov, P. A., and Hammock B. D. (2007). Mass spectrometry-based metabolomics. *Mass Spectrometry Reviews* **26**: 51–78.

Devaux, P.G., Homing, M.G., Homing, B.C. (1971). Benyzloxime derivative of steroids; a new metabolic profile procedure for human urinary steroids. *Analytical Letters* (**4):** 151,.

Dunn, WB. and Ellis, DI. (2005). Metabolomics: Current analytical platforms and methodologies. *Trends in Analytical Chemistry* **24**:285–294.

Dwivedi, P., Bendiak, B., Clowers B. H. & Hill, H. H., Jr. (2007). Rapid resolution of carbohydrate isomers by electrospray ionization ambient pressure ion mobility spectrometry-time-of-flight mass spectrometry (ESI-APIMS-TOFMS). *Journal of the American Society for Mass Spectrometry* **18**: 1163-1175.

Eiceman, G. A. & Karpas, Z. (2005). Ion Mobility Spectrometry. *2nd ed*, CRC Press, Boca Raton, FL, USA, p.3.

Eisenthal, R. & Panes, A. (1985). The aerobic/anaerobic transition of glucose metabolism in *Trypanosoma brucei.* FEBS Letters **181**: 23-27.

Ekman, R., Silberring, J., Westman-Brinkmaln, A., and Kraj, A. (2009). *Mass Spectrometry: Instrumentation and Application*. John Wiely and Sons, USA, pp: 23-24, 27-29, 40-41, 49.

Gavaghan, C. L., Wilson, I. D., & Nicholson, J. K. (2002). Physiological variation in metabolic phenotyping and functional genomic studies: Use of orthogonal signal correction and PLSDA. *FEBS Letters* **530**: 191–196.

Giavalisco, P., Hummel, J., Lisec, J., Inostroza, A. C., Catchpole, G. & Willmitzer, L., (2008). High-resolution direct infusion-based mass spectrometry in combination with whole ^{13}C metabolome isotope labeling allows unambiguous assignment of chemical sum formulas. *Analytical Chemistry* **80**: 9417-9425.

Glassop, D., Roessner, U., Bacic, A. & Bonnett, G. D., (2007). Changes in the sugarcane metabolome with stem development. Are they related to sucrose accumulation? *Plant Cell Physiology* **48**: 573-584.

Guo, Y. & Gaiki S. (2005). Retention behaviour of small polar compounds on polar stationary phases in hydrophilic interaction chromatography. *Journal of Chromatogrraphy A* **1074**:71–80.

Halket, J. M., Waterman, D., Przyborowska, A. M., Patel, R. K., Fraser, P. D. & Bramley, P. M. (2005). Chemical derivatization and mass spectral libraries in metabolic profiling by GC/MS and LC/MS/MS. *Journal of Experimental Botany* **56**: 219-243.

Hammond, D. J. & Bowman, I. B. (1980). *Trypanosoma brucei*: the effect of glycerol on the anaerobic metabolism of glucose. *Molecular and Biochemical Parasitology* **2**: 63-75.

Harrigan, G. G., Maguire, G., and Boro, L. (2008). Metabolomics in Alcohol Research and Drug Development. *Alcohol Research & Health* **31**(1):26-35 .

Havsteen, B. H., (2002). The biochemistry and medical significance of the flavonoids. *Pharmacology and Therapeutics* **96**: 67-202.

Hegeman, A. D., Schulte, C. F., Cui, Q., Lewis, I. A., Huttlin, E. L., Eghbalnia, H., Harms, A. C., Ulrich, E. L., Markley, J. L. & Sussman, M. R. (2007). Stable isotope assisted assignment of elemental compositions for metabolomics. *Analytical Chemistry* **79**: 6912-6921.

Hemstrom, P. & Irgum, K. (2006). Hydrophilic interaction chromatography. *Journal of Separation Science* **29**: 1784-1821.

Higashi, K. O. & de Castro, S. L. (1994). Propolis extracts are effective against *Trypanosoma cruzi* and have an impact on its interaction with host cells. *Journal of Ethnopharmacology* **43**: 149-155.

Horning, B.C. & Homing, M.G. (1970). Metabolic Profiles: chromatographic methods for isolation and characterization of a variety of metabolites in man. In Methods in Medical Research (Olsen, R.E. Ed.) 369 (Yearbook Medical Publishers, Chicago.

Horning, E.C. & Homing, M.G (1971). Human metabolic profiles obtained by GC and GC/MS. *Journal of Chromatographic Science* **9**: 129-140.

Hu, Q., Noll, R. J., Makarov, H. Li, A., Hardman, M. & R. Graham Cooks, (2005) The Orbitrap: a new mass spectrometer. *Journal of Mass Spectrometry* **40**: 430-443.

Hubschmann, H. (2009). Handbook of Gc/MS:Fundamentals and Applications. 2nd ed, Wiley-VCH Verlag GmbH & Co. KGaA, Weinheim, Germany, pp:206-208.

Johnstone D. B. (1961). Growth of Azobacter in deuterium oxide. *Journal of Bacteriology* **83**(4): 867-870.

Jones, D. C., Ariza, A., Chow, W. H., Oza, S. L. & Fairlamb, A. H. (2010). Comparative structural, kinetic and inhibitor studies of *Trypanosoma brucei* trypanothione reductase with T. cruzi. *Mol Biochem Parasitol* **169**: 12-19.

Kamleh, A., Barrett, M. P., Wildridge, D., Burchmore, R. J., Scheltema, R. A. & Watson, D. G. (2008). Metabolomic profiling using Orbitrap Fourier transform mass spectrometry with hydrophilic interaction chromatography: a method with wide applicability to analysis of biomolecules. *Rapid Communications in Mass Spectrometry* **22**: 1912-1918.

Keun, H. C., Ebbels, T. M., Antti, H. M., Bollard, E., Beckonert, O., Schlotterbeck, G., Senn, H., Niederhauser, U., Holmes, E., Lindon, J. C. & Nicholson, J. K. (2002). Analytical reproducibility in (1)H NMR-based metabonomic urinalysis. *Chemical Research in Toxicology* **15**: 1380-1386.

Kopka, J., (2006). Current challenges and developments in GC-MS based metabolite profiling technology. *Journal of Biotechnology* **124**: 312-322.

Krishnan, P., Kruger, N. J. & Ratcliffe, R. G. (2004). Metabolite fingerprinting and profiling in plants using NMR. *Journal of Experimental Botany* **56**(410): 255–265.

Makarov, A, Denisov, E, Kholomeev, A, Balschun, W, Lange, O, Strupat, K, Horning, S. (2006a). Performance evaluation of a hybrid linear ion trap/ orbitrap mass spectrometer. *Analytical Chemistry* **78**:2113–2120.

Makarov, A.A., Denisov, E., Lange & O. Horning, S.(2006b). Dynamic range of mass accuracy in LTQ orbitrap hybrid mass spectrometer. *Journal of American Society for Mass Spectrometry* **17**:977–982.

Marcucci, MC. (1995). Propolis: chemical composition, biological properties and therapeutic activity. *Apidologie* **26**: 83–99.

Marley, J., M. Lu & C. Bracken, (2001) A method for efficient isotopic labeling of recombinant proteins. *Journal of Biomolecular NMR* **20**: 71-75.

Marr, J. & Muller, M. (1995). *Biochemistry and Molecular Biology of Parasites*. 1st ed, Academic Press, UK, pp: 19-26, 33-45, 67-79.

Martins, R. M., Covarrubias, C., Rojas, R. G., Silber, A. M. & Nobuko Yoshida (2009). Use of L-Proline and ATP Production by *Trypanosoma cruzi* Metacyclic Forms as Requirements for Host Cell Invasion. *Infection and Immunity* **77(**7): 3023–3032.

Michels, P. A., Bringaud, F., Herman, M. & Hannaert, V. (2006) Metabolic functions of glycosomes in trypanosomatids. *Biochimica Biophysica Acta* **1763**: 1463-1477.

Milne, K. G., Prescott, A. R. & Ferguson, M. A. (1998) Transformation of monomorphic *Trypanosoma brucei* bloodstream form trypomastigotes into procyclic forms at 37 degrees C by removing glucose from the culture medium. *Molecular and Biochemical Parasitology* **94**: 99-112.

Minkler, P.E., Kerner, J., Kasumov, T., Parland, W., and Hoppel, C.L. (2006). Quantification of malonyl-coenzyme A in tissue specimens by high-performance liquid chromatography/ mass spectrometry. *Analytical Biochemistry* **352:** 24-32.

Miyata R. & Yonehara T. (1996). "Improvement of Fermentative Production of Pyruvate from Glucose by *Torulopsis glabrata*". *Journal of Fermentation and Bioengineering* **82**(5): 475-479.

Monton, M. R. & Soga, T. (2007) Metabolome analysis by capillary electrophoresis-mass spectrometry. *Journal of Chromatography A* **1168**: 237-246.

Mroczek, W.J, (1972) Biochemical profiling and the natural history of hypertensive diseases. *Circulation* **45**: 1332-1333.

Nevo, A. N., Pshenichnikova, A. B., Skladnev, D. A. & Shvets, V. I. (2004). Deuterium oxide as a stress factor to the methylotrophic bacterium *Methylophilus sp.*. *Micobiology* **73**: 175-179.

Nolan, D. P., Rolin, S., Rodriguez, J. R., Van Den Abbeele, J. & Pays, E. (2000). Slender and stumpy bloodstream forms of *Trypanosoma brucei* display a differential response to extracellular acidic and proteolytic stress. *European Journal of Biochemistry* **267**: 18-27.

Ohta, D., Kanaya, S. & Suzuki, H. (2010). Application of Fourier-transform ion cyclotron resonance mass spectrometry to metabolic profiling and metabolite identification. *Current Opinion in Biotechnology* **21**: 35-44.

Overath, P., Czichos, J. & Haas, C. (1986). The effect of citrate/cis-aconitate on oxidative metabolism during transformation of *Trypanosoma brucei*." *European Journal of Biochemistry* **160**(1): 175-82.

Priest, J. W. & Hajduk, S. L. (1994). Developmental regulation of mitochondrial biogenesis in *Trypanosoma brucei*. *Journal of Bioenergetics and Biomembranes* **26:** 179-191.

Queiroz, R., Benz, C., Fellenberg, K., Jörg D Hoheisel, J. D. & Clayton, C. (2009). Transcriptome analysis of differentiating trypanosomes reveals the existence of multiple post-transcriptional regulons. *BMC Genomics* **10**:495.

Ramautar, R., Somsen, G. W. & de Jong, G. J. (2007). Direct sample injection for capillary electrophoretic determination of organic acids in cerebrospinal fluid. *Analytical and Bioanalytical Chemistry* **387**: 293-301.

Rolin, S., Hancocq-Quertier, J., Paturiaux-Hanocq, F., Nolan, D. P. & Pays, E. (1998). Mild acid stress as a differentiation trigger in *Trypanosoma brucei*. *Molecular and Biochemical Parasitology* **93**: 251-262.

Sariyar-Akbulut, B., Salman-Dilgimen, A., Ceylan, S. , Perk, S., Denizci A. A. & Kazan D. (2008). Preliminary phenotypic characterization of newly isolated halophilic microorganisms by footprinting: a rapid metabolome analysis. *Archives of Microbiology* **189**:19–26.

Saunders, E. C., De Souza, D. P., Naderer, T., Sernee, M. F., Ralton, J. E., Doyle, M. A., Macrae, J. I., Chambers, J. L., Hen,g J., Nahid, A., Likic, V. A. & Mcconville, M. J. (2009). Central carbon metabolism of Leishmania parasite. *Parasitology* **137**(9):1303-13.

Saur, W. K., Crespi, H. L., Halevi, E. A. & Katz, J. J. (1968). Deuterium isotope effects in the fermentation of hexoses to ethanol by *Saccharomyces cerevisiae. I*. Hydrogen exchange in the glycolytic pathway. *Biochemistry* **7**: 3529-3536.

Sawada, Y., Akiyama, K., Sakata, A., Kuwahara, A., Otsuki, H., Sakurai, T., Saito, K. & Hirai, M. Y. (2009). Widely targeted metabolomics based on large-scale MS/MS data for elucidating metabolite accumulation patterns in plants. *Plant Cell Physiology* **50**: 37-47.

Sawaya, A. C. H. F., Cunha, I. B. S., Marcucci, M. C., Aidar, D. S., Silva E. C. A., Carvalho C. A. L.& Eberlin M. N.(2007). Electrospray ionization mass spectrometry fingerprinting of propolis of native Brazilian stingless bees. *Apidologie* 38: 93–103.

Seidel, V., Peyfoon, E., Watson, D. G. & Fearnley, J. (2008). Comparative study of the antibacterial activity of propolis from different geographical and climatic zones. *Phytotherapy Research* **22**: 1256-1263.

Shellie, R. A., Welthagen, W., Zrostlikova, J., Spranger, J., Ristow, M., Fiehn, O. & Zimmermann, R. (2005). Statistical methods for comparing comprehensive two-dimensional gas chromatography-time-of-flight mass spectrometry results: metabolomic analysis of mouse tissue extracts. *Journal of Chromatography A* **1086**: 83-90.

Sowers, K. R. & Gunsalus, R. P. (1995). Halotolerance in *Methanosarcina spp.*: Role of Ne-Acetylb-Lysine, a-Glutamate, Glycine Betaine, and K1 as Compatible Solutes for Osmotic Adaptation. *American Society for Microbiology* **61**(12): 4382–4388.

Spinks, D., Shanks, E. J., Cleghorn, L. A., McElroy, S., Jones, D., James, D., Fairlamb, J. A. Frearson, A. H., Wyatt, P. G. & Gilbert, I. H. (2009). Investigation of trypanothione reductase as a drug target in *Trypanosoma brucei. ChemMedChem* **4**: 2060-2069.

Spitznagel, D., Ebikeme, C., Biran, M., Bhaird, Bringaud, F., Henehan, G. T. M. & Nolan, D. P. (2009). Alanine aminotransferase of *Trypanosoma brucei* – a key

role in proline metabolism in procyclic life forms. *FEBS Journal* 267 (23):7187-99.

Stoyanova, R., & Brown, T. R. (2001). NMR spectral quantitation by principal component analysis. *NMR in Biomedicine* **14**: 271–277.

Strange, K. (2004) Cellular volume homeostasis. *Advances in Physiology Education* **28**: 155-159.

Tyler, K.M., Matthews, K.R., & Gull, K. (1997). The bloodstream differentiation-division of *Trypanosoma brucei* studied using mitochondrial markers. *Proceedings. Biological sciences* **264:** 1481-1490.

Uzcategui, N. L., Carmona-Gutierrez, D., Denninger, V., Schoenfeld, C., Lang, F., Figarella, K. & Duszenko, M. (2007). Antiproliferative effect of dihydroxyacetone on *Trypanosoma brucei* bloodstream forms: cell cycle progression, subcellular alterations, and cell death. *Antimicrobial Agents and Chemotherapy* **51**: 3960-3968.

van Grinsven, K. W., Van Den Abbeele, J., Van den Bossche, P., van Hellemond, J. J. & Tielens, A. G. (2009). Adaptations in the glucose metabolism of procyclic *Trypanosoma brucei* isolates from tsetse flies and during differentiation of bloodstream forms. *Eukaryotic Cell* **8**: 1307-1311.

van Hellemond, J. J., Hoek, A., Schreur, P. W., Chupin, V., Ozdirekcan, S., Geysen, D., van Grinsven, K. W., Koets, A. P., Van den Bossche, P., Geerts, S. & Tielens, A. G. (2007). Energy metabolism of bloodstream form *Trypanosoma theileri. Eukaryotic Cell* **6**: 1693-1696.

Vassella, E., Reuner, B., Yutzy, B. & Boshart, M. (1997). Differentiation of African trypanosomes is controlled by a density sensing mechanism which signals cell cycle arrest via the cAMP pathway. *Journal of Cell Science* 110 (Pt 21): 2661-2671.

Viant, M. R. (2009) Applications of metabolomics to the environmental sciences. Metabolomics. *Springer Science and Business Media* **5**:1–2, US.

Volpi, N. & Bergonzini, G. (2006). Analysis of flavonoids from propolis by on-line HPLC-electrospray mass spectrometry. *Journal of Pharmaceutical and Biomedical Analysis* **42**: 354-361.

Wiemer, E.A., Michels, P.A., and Opperdoes, F.R. (1995). The inhibition of pyruvate transport across the plasma membrane of the bloodstream form of *Trypanosoma brucei* and its metabolic implications. *Biochemical Journal* **312** (Pt 2): 479-484.

Wilson, I. D., Plumb, R., Granger, J., Major, H., Williams, R. & Lenz, E. M. (2005). HPLC-MS-based methods for the study of metabonomics. *Journal of Chromatography B Analytical Technologies in the Biomedical Life Sciences* **817**: 67-76.

Wu, Z., Huang, Z., Lehmann, R., Chunxia Zhao, C. & Xu, G. (2009). The Application of Chromatography-Mass Spectrometry: Methods to Metabonomics. *Chromatographia* **69**(supp1):23-32

Zamboni, N. & Sauer, U. (2009). Novel biological insights through metabolomics and 13C-flux analysis. *Current Opinion in Microbiology* **12**: 553-558.

Zamboni, N., Fendt, S. M. , Ruhl, M. & Sauer, U. (2009) (13)C-based metabolic flux analysis. *Nature Protocols* **4**: 878-892.

Zhang, X., Wang, Y., Hao, F., Zhou, X., Han, X., Tang, H. & Ji, L. (2009). Human serum metabonomic analysis reveals progression axes for glucose intolerance and insulin resistance statuses. *Journal of Proteome Research* **8**: 5188-5195.

APPENDICES

Appendix I: Glycolysis as described in the KEGG database.

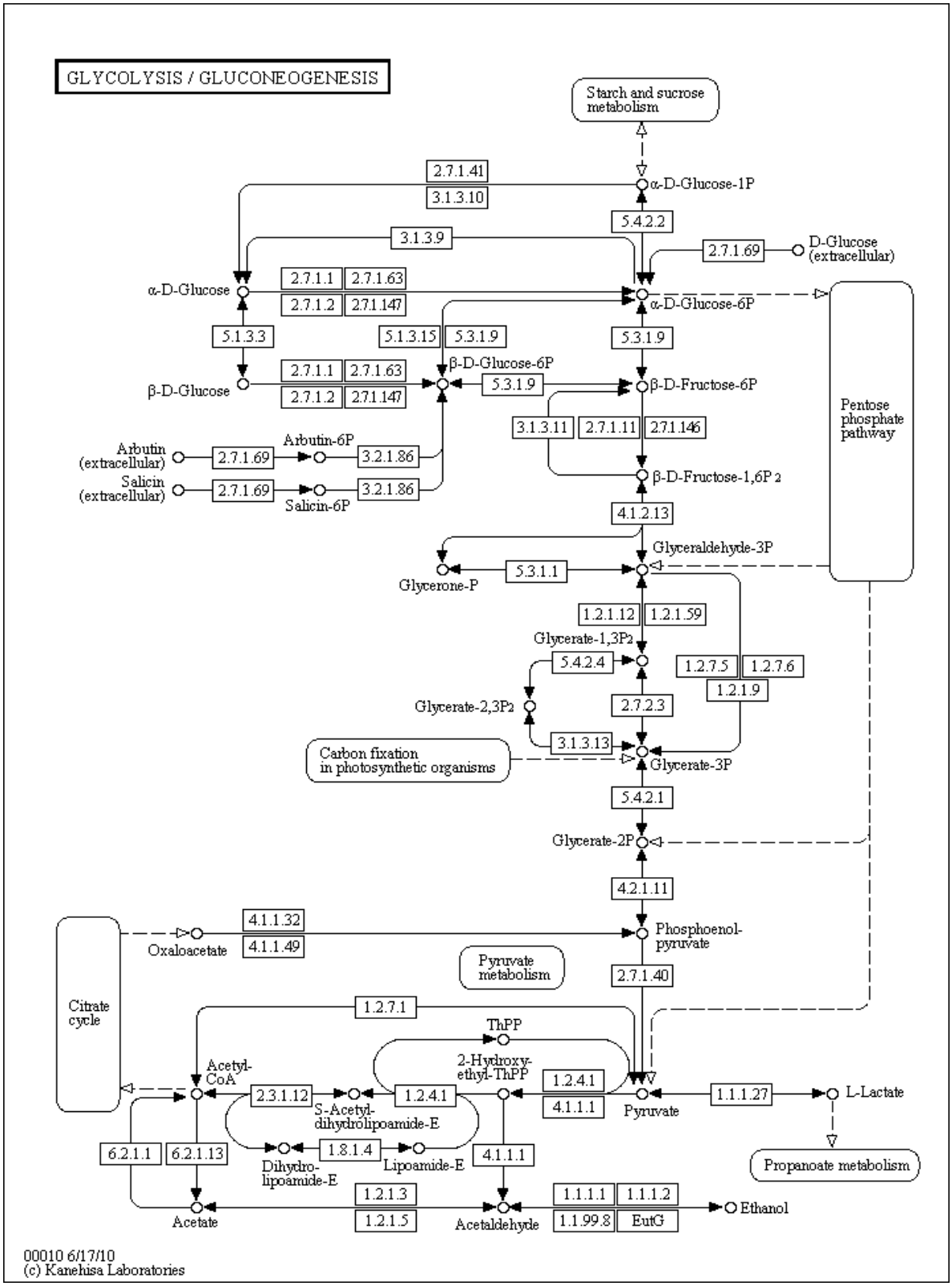

Appendix II: pyruvate metabolism as described in the KEGG database.

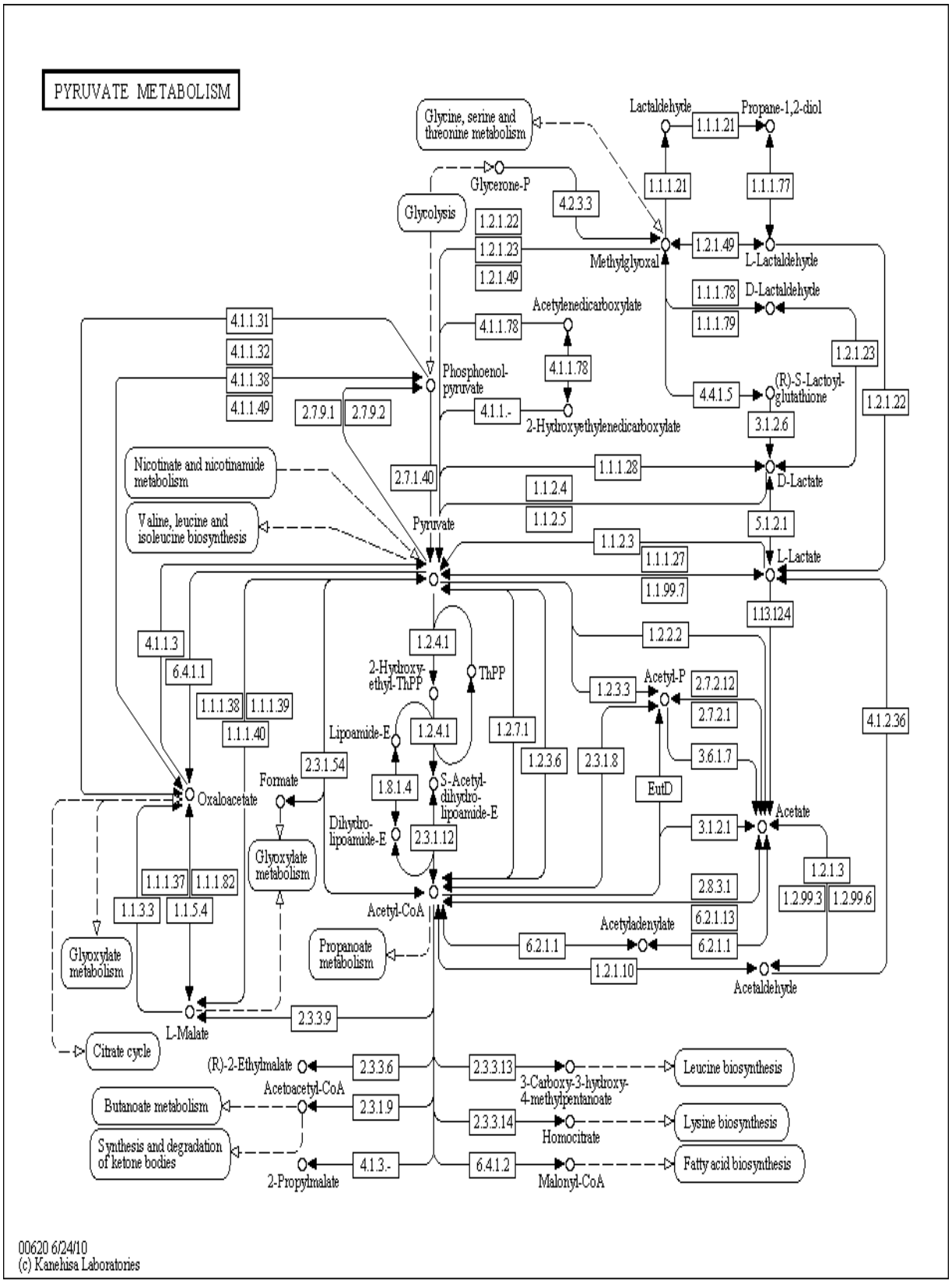

Appendix III: Propanoate metabolism as described in the KEGG database.

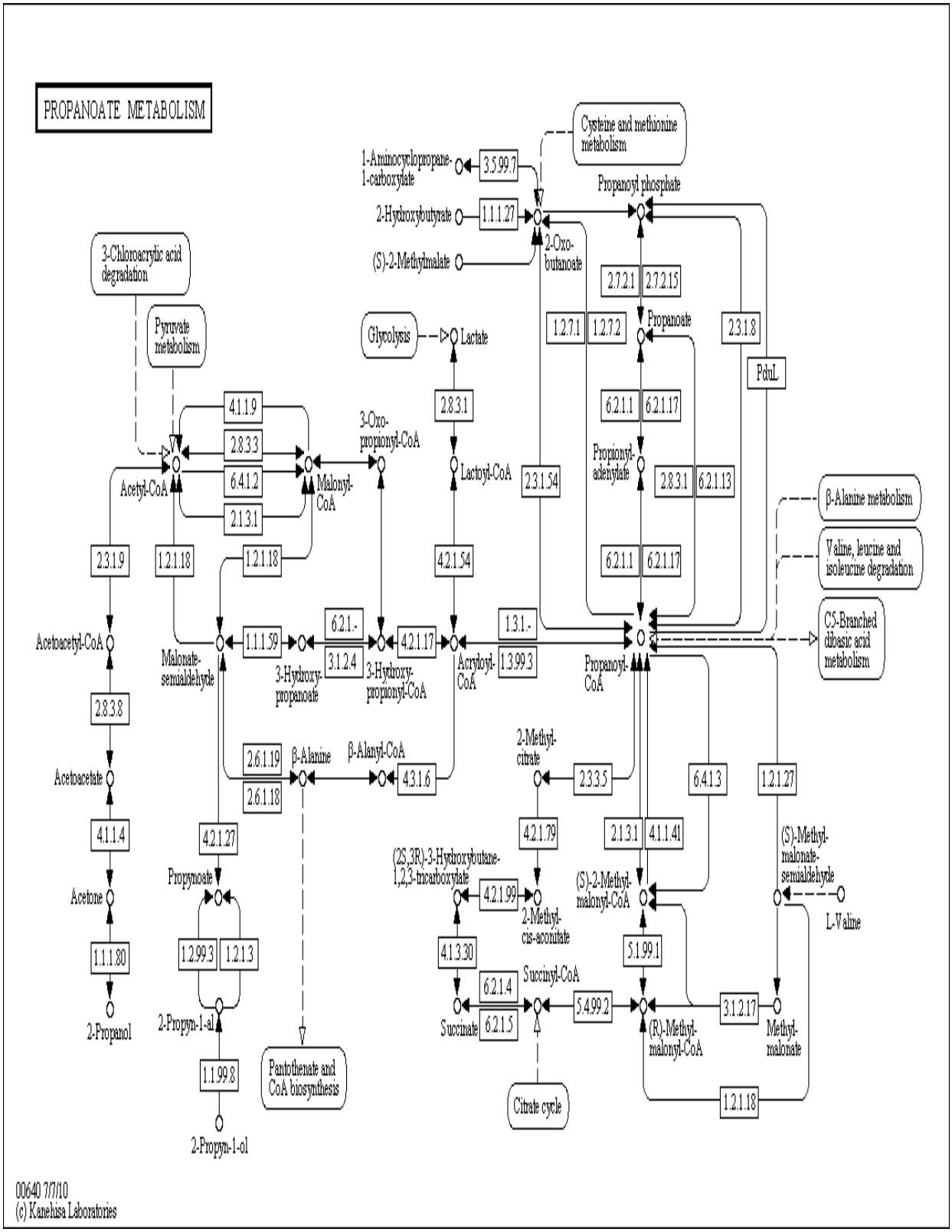

Appendix IV: Pentose phosphate pathway as described in the KEGG database.

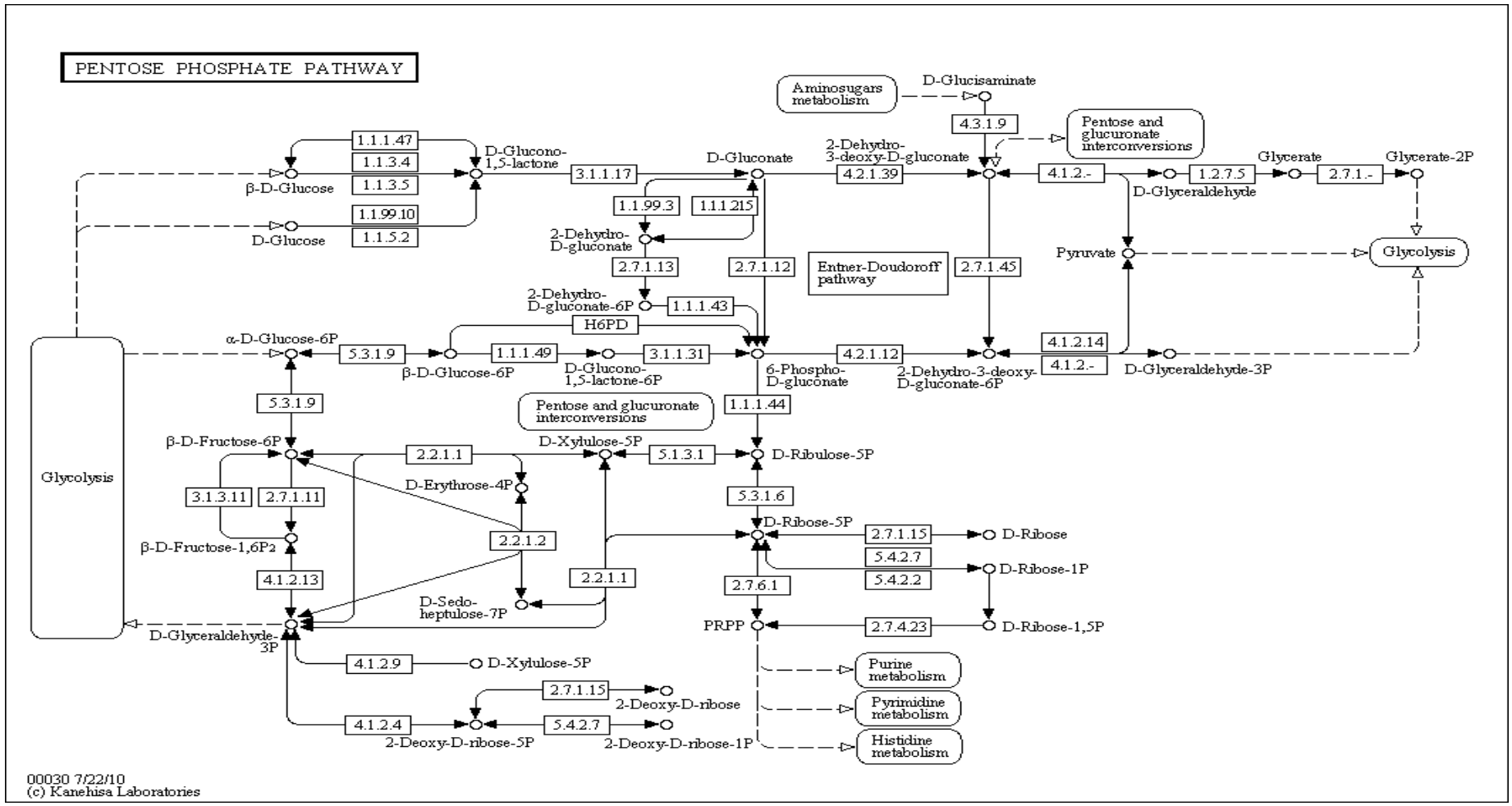

Appendix V: Kreb's Cycleas described in the KEGG database.

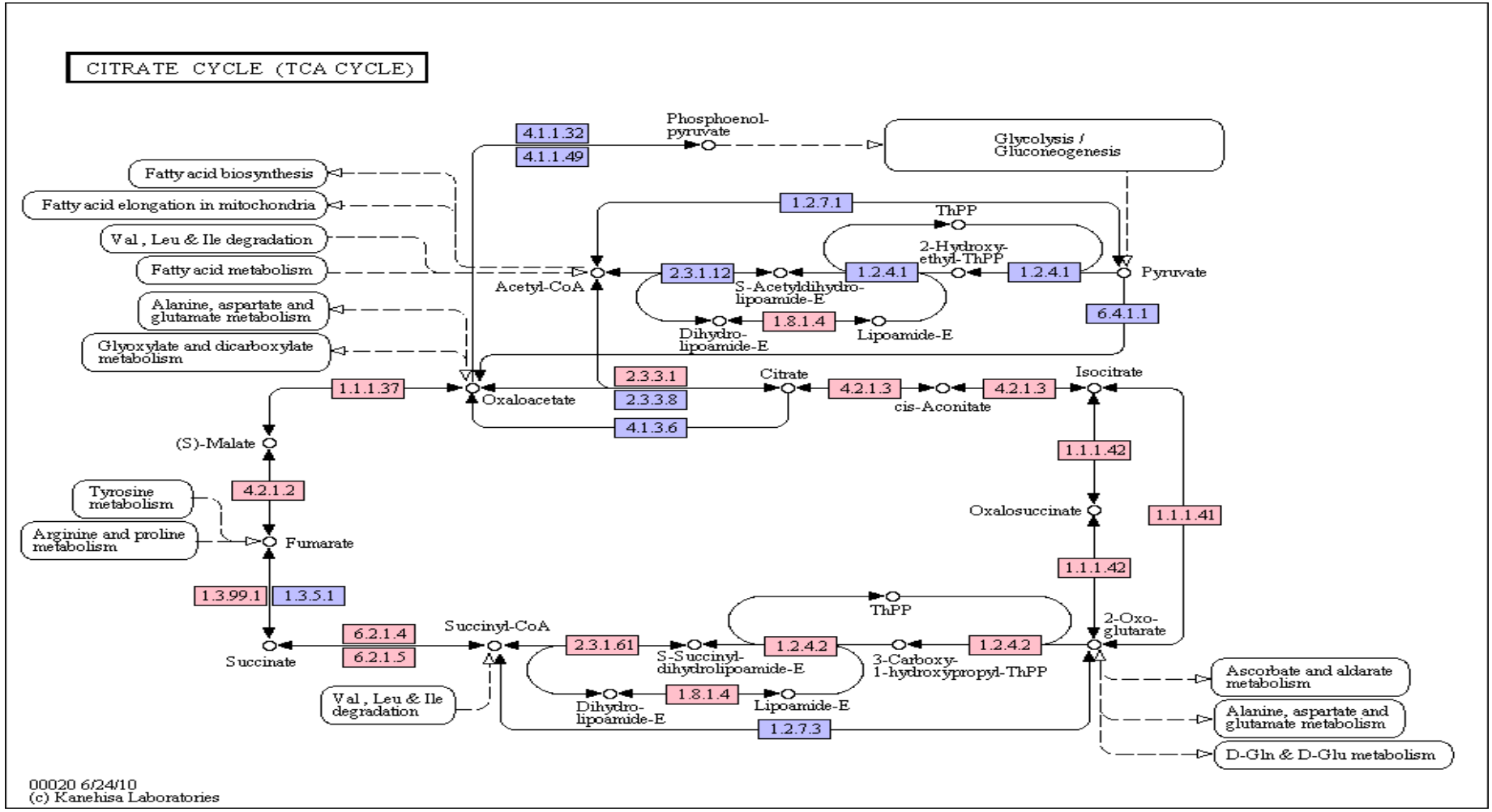

Appendix VI: MS^2 spectra for succinic acid (A) and $^{13}C_3$ succinic acid (B).